

MICROCOPY RESOLUTION TEST CHART
NATIONAL BUREAU OF STANDARDS-1963-A

LEVEL II

✓ 79-182.T

①
B.S.

AD A 091459

DETERMINATION OF MODAL PARAMETERS FROM
EXPERIMENTAL FREQUENCY RESPONSE DATA

DTIC
ELECTE
NOV 12 1980
E

APPROVED:

Wing C. Smith
Walter S. Reed

DDC FILE COPY

DISTRIBUTION STATEMENT A
Approved for public release;
Distribution Unlimited

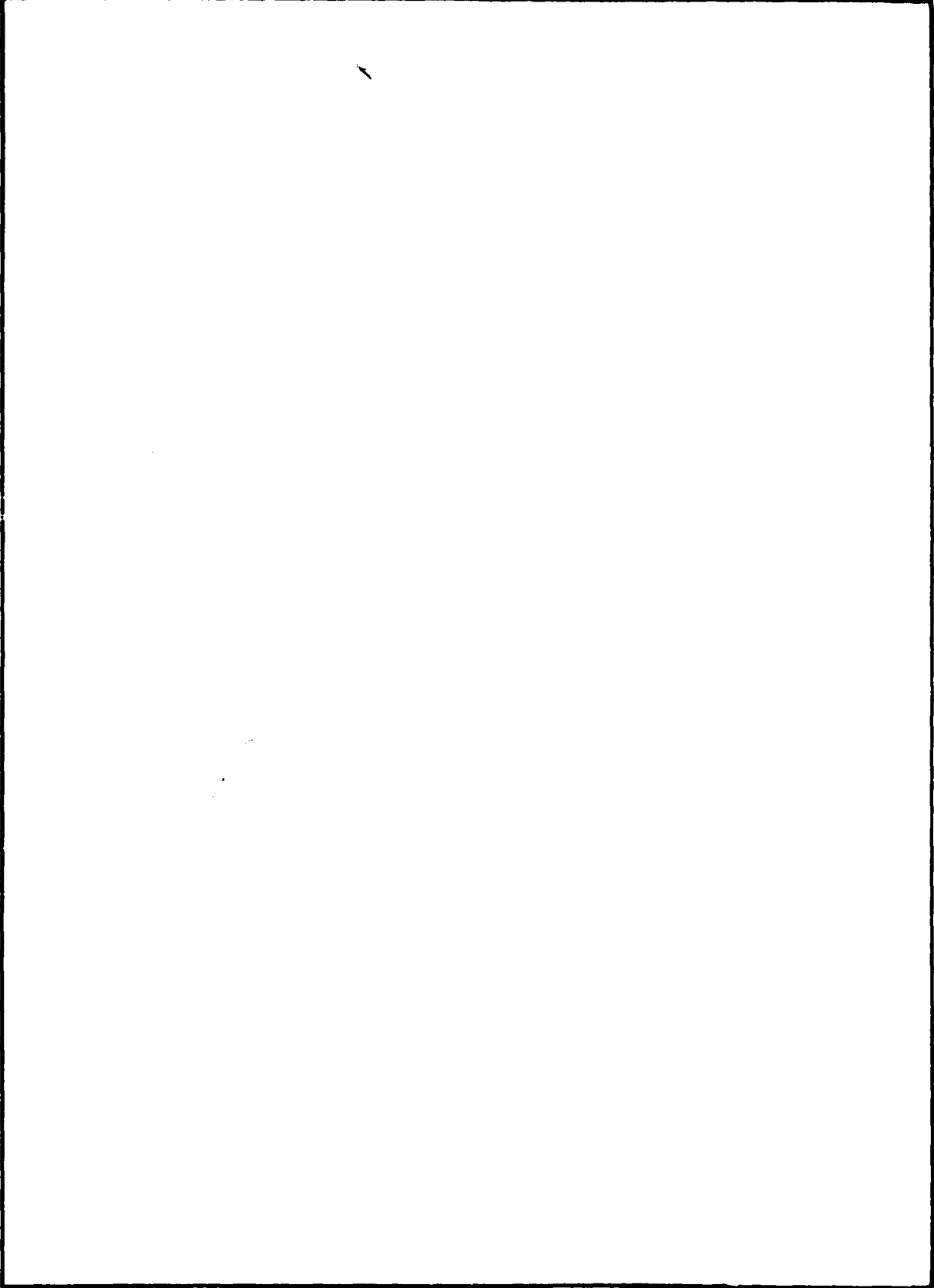
80 16 16 390

UNCLASSIFIED

SECURITY CLASSIFICATION OF THIS PAGE (When Data Entered)

REPORT DOCUMENTATION PAGE		READ INSTRUCTIONS BEFORE COMPLETING FORM
1. REPORT NUMBER 79-182T	2. GOVT ACCESSION NO. AD-A091 459	3. RECIPIENT'S CATALOG NUMBER 14 AFIT-CI-79-182T
4. TITLE (and Subtitle) Determination of Modal Parameters from Experimental Frequency Response Data	5. TYPE OF REPORT & PERIOD COVERED Thesis	
7. AUTHOR(s) Clarence Walter Miller		6. PERFORMING ORG. REPORT NUMBER
9. PERFORMING ORGANIZATION NAME AND ADDRESS AFIT student at: The University of Texas at Austin		8. CONTRACT OR GRANT NUMBER(s) Master's thesis
11. CONTROLLING OFFICE NAME AND ADDRESS AFIT/NR WPAFB OH 45433	10. PROGRAM ELEMENT, PROJECT, TASK AREA & WORK UNIT NUMBERS	
14. MONITORING AGENCY NAME & ADDRESS (if different from Controlling Office)		12. REPORT DATE Dec 1978
		13. NUMBER OF PAGES 127
		15. SECURITY CLASS. (of this report) Unclassified
		15a. DECLASSIFICATION/DOWNGRADING SCHEDULE
16. DISTRIBUTION STATEMENT (of this Report) Approved for public release; distribution unlimited		
17. DISTRIBUTION STATEMENT (of the abstract entered in Block 20, if different from Report) APPROVED FOR PUBLIC RELEASE AFR 190-17. Fredric C. Lynch FREDRIC C. LYNCH, Major, USAF Director of Public Affairs		
18. SUPPLEMENTARY NOTES Air Force Institute of Technology (ATC) Wright-Patterson AFB, OH 45433		
19. KEY WORDS (Continue on reverse side if necessary and identify by block number)		
20. ABSTRACT (Continue on reverse side if necessary and identify by block number) Attached		

SECURITY CLASSIFICATION OF THIS PAGE(When Data Entered)



SECURITY CLASSIFICATION OF THIS PAGE(When Data Entered)

ABSTRACT

In recent years, a number of advances have been made in determining the dynamic properties of a structure. These advances have opened the field of modal analysis, the term used to describe the use of experimental frequency response data to determine the modal properties of natural frequencies, damping ratios, and mode shapes. One of the main problems in the area of modal analysis is the lack of complete documentation for the techniques in use. The purpose of this thesis is to investigate some of the modal analysis techniques in use, and to document, fully, the assumptions and the equations and computer algorithms associated with each method. Three curve fitting techniques are presented along with some example problems which demonstrate the limitations of each method.

DETERMINATION OF MODAL PARAMETERS FROM
EXPERIMENTAL FREQUENCY RESPONSE DATA

by

CLARENCE WALTER MILLER, B.S.A.S.E.

THESIS

Presented to the Faculty of the Graduate School of
The University of Texas at Austin

in Partial Fulfillment
of the Requirements
for the Degree of

MASTER OF SCIENCE IN ENGINEERING

Accession For	
NTIS GRA&I	<input checked="" type="checkbox"/>
DDC TAB	<input type="checkbox"/>
Unannounced	<input type="checkbox"/>
Justification	<input type="checkbox"/>
By _____	
Distribution/ _____	
Availability Codes	
Dist..	Avail and/or special
A	

THE UNIVERSITY OF TEXAS AT AUSTIN

December 1978

ACKNOWLEDGEMENTS

The author would like to express his gratitude for the assistance of Dr. Craig Smith throughout this project. His insight and guidance were invaluable. Also of considerable help were the comments of Joe Thornhill of IBM.

The author would also like to thank Capt. Samuel Brown of the Air Force Institute of Technology for his efforts in the management of the author's education program.

C. W. M.

December, 1978

TABLE OF CONTENTS

	Page
ACKNOWLEDGEMENTS	iii
ABSTRACT	iv
CHAPTER	
I. INTRODUCTION	1
II. THE STRUCTURAL DYNAMIC MODEL	7
2.1 Assumptions	7
2.2 The Transfer Matrix	8
2.3 Modes of Vibration	10
2.4 Complex Mode Shapes	17
2.5 Deriving Mass, Stiffness, and Damping Matrices From Frequency Response Data	19
2.6 Summary	24
III. MODAL PARAMETER ESTIMATION TECHNIQUES	26
3.1 Parameter Identification	26
3.2 Single Degree of Freedom Techniques	29
3.2.1 Quadrature Response Technique	29

	Page
3.2.2 Method of Kennedy and Pancu	32
3.3 Multi Degree of Freedom Curve Fitting	46
3.3.1 Complex Curve Fit	46
3.3.2 Curve Fitting of Quadrature Response	57
3.4 Summary	63
IV. EXAMPLES OF CURVE FITTING TECHNIQUES . . .	64
4.1 Introduction	64
4.2 Example Problem One	65
4.2.1 Method of Kennedy and Pancu	66
4.2.2 Complex Curve Fit	71
4.2.3 Curve Fit of Imaginary Part of $H(j\omega)$	73
4.3 Example Problem Two	76
4.3.1 Method of Kennedy and Pancu	77
4.3.2 Complex Curve Fit	84
4.3.3 Curve Fit of Imaginary Part of $H(j\omega)$	85
4.4 Determination of Mass, Stiffness, and Damping Matrices	87
4.5 Summary	89
V. SUMMARY AND CONCLUSIONS	91

Page

APPENDIX A - CIRCLE FIT ALGORITHM	96
APPENDIX B - MULTI DEGREE OF FREEDOM CURVE FIT ALGORITHM	101
APPENDIX C - IMAGINARY CURVE FIT ALGORITHM	105
APPENDIX D - DATA	111
BIBLIOGRAPHY	127
VITA	

CHAPTER I

INTRODUCTION

The use of experimental methods to determine the dynamic characteristics of a system or structure has become widely used and accepted during the 1970's, primarily because of the advances in digital test equipment. The use of these methods has become commonly known as modal analysis. Experimental modal analysis provides the ability to pinpoint vibration problems by showing troublesome frequencies, damping factors, and mode shape data which can be used by a designer to pinpoint weak spots in a structure.

In order to obtain meaningful answers to vibration problems, it is essential that an adequate mathematical model be selected. If a model is available, there are methods which can be used for computing the dynamic response of the structure. However, if the parameters, i.e., mass, stiffness, and damping, are not known, or if the model itself is not known, then the solutions cannot be obtained. One approach to modeling is through the use of transfer functions. If the applicable transfer functions can be determined,

then the response to any input can be determined. One advantage in using the transfer function approach is that only those points of a structure which are of interest need be considered. The determination of these transfer functions is the main thrust in experimental modal analysis.

In general, modal analysis involves the description of the dynamic characteristics of a structure by observing its natural modes of vibration and the associated modal properties, i.e., frequency and damping ratio. Natural frequency and damping ratio are global properties of the system and consequently can be measured at almost any point on the system. The key to reliable modal parameter estimates is the accurate measurement of transfer functions of the system. The transfer function is a complex valued function. The Laplace transform is used to characterize the transfer function because it can be used to convert a measured frequency response function into a partial fraction expansion with each partial fraction containing information on each resonance of the system in the frequency range of analysis. The frequency response function, which is the ratio of the output to the input (assumed here to be the ratio of output dis-

placement to input force) evaluated along the $j\omega$ frequency axis, can be used to determine the frequency, damping, magnitude, and phase of each resonance.

The purpose of this thesis is not to describe the techniques used in obtaining the frequency response function, but rather to explore three methods of extracting the modal parameters from the measured data and to point out the advantages and disadvantages of each method. For a description on frequency response measurement techniques in mechanical systems, the reader is directed to references (10) and (11).¹

For a brief review of the literature, prior to 1968, concerning the modeling, or measuring, of the transfer function, the reader is referred to a PhD dissertation by William R. Shapton, (15). Shapton discusses briefly the problems with earlier attempts at transfer function measurement. Some of the earlier works reviewed by Shapton include Savant (14), Chestnut and Mayer (2), Crafton (3), Tse, Morse, and Hinkle (17), Jacobsen and Ayre (5), Brooks (1), Simmons (16), and many others. Shapton's work was

¹From this point on, the nomenclature () will be used to denote a reference number in the bibliography.

in the development of procedures for predicting the response versus time of surface strain of a complex structure resulting from a dynamic excitation. His assumptions were that the structure was capable of being represented as a linear system with time invariant parameters, and that the system could be approximated by a finite number of ordinary differential equations with constant coefficients. He also assumed that the system was underdamped and that the damping could be represented as an equivalent viscous damping. Shapton presents a method to determine the transfer function by extracting it in analytical form from the experimentally determined frequency response data.

Most of the works performed in the area of deriving transfer functions from experimental data have as their initial basis, a method presented by Kennedy and Pancu (6). Kennedy and Pancu presented one of the first papers on determining modal characteristics from test data. The object of their paper was to bring out an awareness of the phase relationship in trying to correlate between measured and calculated modes. They presented a technique to identify normal modes from polar plots (plot of re-

response vector with forcing frequency) of the frequency response function. The basis for this technique is that near a resonant frequency the polar plot will approximately describe a circle (for a single mode). This method will be discussed further in a later section of this thesis.

A more recent work in this area was done by Klosterman (8). He presented new methods to determine a complex modal representation from experimental data. He generalized the method of Kennedy and Pancu to include the case where damping is not proportional to the stiffness or mass.

Using Klosterman's work, more recent papers by Richardson (11) and Potter and Richardson (9) have presented the basis for measuring transfer functions using a least squares estimator to measured frequency response data.

This thesis will discuss the circle fit method of Kennedy and Pancu, and two other curve fit techniques, one which uses the total response curve, and one which uses only the imaginary part of the response. Chapter II presents the dynamic model used for an elastic structure and the compliance transfer function for the structure in the Laplace

domain. Chapter III discusses four methods of extracting the desired modal parameters from the frequency response function. Chapter IV will present two example problems using three of the methods discussed in Chapter III. And finally, Chapter V is the summary and conclusions of the methods discussed.

CHAPTER II
THE STRUCTURAL DYNAMIC MODEL

2.1 Assumptions

In most problems in modal analysis, the model is assumed to be described by a system of n simultaneous second order linear differential equations. In the time domain these equations are given by

$$\underline{M} \ddot{\underline{x}} + \underline{C} \dot{\underline{x}} + \underline{K} \underline{x} = \underline{f} (t) \quad (2.1)$$

where

$\underline{x} (t)$ = n -dimensional displacement vector

$\underline{f} (t)$ = n -dimensional force vector

\underline{M} = $n \times n$ mass matrix

\underline{C} = $n \times n$ damping matrix

\underline{K} = $n \times n$ stiffness matrix

For the purpose of this thesis, it is assumed that the matrices \underline{M} , \underline{C} , and \underline{K} are real valued and symmetric. The energy associated with the mass and stiffness matrices is stored and can always be recovered, however, the energy associated with the damping is dissipated and is lost from the system.

The damping mechanism in this formulation is assumed to be viscous, i.e., damping force is proportional to velocity. In practice, most mechanical structures exhibit rather complicated damping mechanisms, however, Richardson and Potter (13) have shown that all of the damping mechanisms can be modeled in terms of energy dissipation by an equivalent viscous damper.

2.2 The Transfer Matrix

The Laplace transform of equation (2.1) yields

$$\underline{M} \left[s^2 \underline{X}(s) - s \underline{x}(0) - \underline{\dot{x}}(0) \right] + \underline{C} \left[s \underline{X}(s) - \underline{x}(0) \right] + \underline{K} \underline{X}(s) = \underline{F}(s) \quad (2.2)$$

Assuming that the initial conditions are zero (or alternately combine them with $\underline{F}(s)$), the transformed equations become

$$\left[\underline{M}s^2 + \underline{C}s + \underline{K} \right] \underline{X}(s) = \underline{F}(s) \quad (2.3)$$

Defining $\underline{B}(s)$ as the system matrix,

$$\underline{B}(s) = \underline{M}s^2 + \underline{C}s + \underline{K} \quad (2.4)$$

then equation (2.3) can be written as

$$\underline{B}(s) \underline{X}(s) = \underline{F}(s) \quad (2.5)$$

$\underline{B}(s)$ is often referred to as the dynamic flexibility of the structure.

Now define $\underline{H}(s)$ as the inverse of $\underline{B}(s)$ (assuming that the inverse exists). Then equation (2.5) becomes

$$\underline{X}(s) = \underline{H}(s) \underline{F}(s) \quad (2.6)$$

$\underline{H}(s)$ is the $n \times n$ transfer matrix, each element of which is a transfer function, i.e., h_{ij} is the transfer function which relates the response at point i due to an excitation at point j . Because of reciprocity $h_{ij} = h_{ji}$ for all i and j . Taking a closer look at each element of $\underline{H}(s)$ reveals that each is a rational fraction in s , i.e.,

$$h_{ij} = \frac{b_1 s^{2n-2} + b_2 s^{2n-3} + \dots + b_{2n-2} s + b_{2n-1}}{\det \underline{B}(s)} \quad (2.7)$$

where

$$\det \underline{B}(s) = \text{determinant of } \underline{B}(s)$$

The roots of $\det \underline{B}(s)$ are called the poles of $\underline{H}(s)$ and are the values of s for which $\det \underline{B}(s) = 0$.

If we assume that the poles of $\underline{H}(s)$ are dis-

tinct, i.e., each of multiplicity one, and that all modes are underdamped, each element of $\underline{H}(s)$ can be expanded into a partial fraction form to give

$$\underline{H}(s) = \sum_{k=1}^n \frac{\underline{A}_k}{s - s_k} + \frac{\underline{A}_k^*}{s - s_k^*} \quad (2.8)$$

where

$s_k = k^{\text{th}}$ pole of $\underline{H}(s)$

$s_k^* = \text{complex conjugate of } s_k$

$\underline{A}_k = \text{complex residue matrix of } \underline{H}(s) \text{ evaluated at } s = s_k$

$\underline{A}_k^* = \text{complex conjugate of } \underline{A}_k$

Each \underline{A}_k can be found by multiplying $\underline{H}(s)$ by $(s - s_k)$ and then evaluating the result at $s = s_k$, as long as the poles are distinct.

2.3 Modes of Vibration

The resonant poles are the locations where $s = s_k$. These poles can be expressed as

$$s_k = -\sigma_k + j\omega_k$$

where

σ_k = the modal damping coefficient of the
 k^{th} mode

ω_k = the damped natural frequency of the
 k^{th} mode

The undamped natural frequency is given by

$$\Omega_k = \sqrt{\sigma_k^2 + \omega_k^2}$$

and the damping ratio is given by

$$\zeta_k = \frac{\sigma_k}{\Omega_k}$$

Each complex conjugate pair of poles (s_k and s_k^*) corresponds to a mode of vibration in the structure. Figure 2.1 shows the poles for a single degree of freedom system as viewed looking down on the s -plane.

Modal vectors, or mode shapes, are defined as solutions to the homogeneous equation

$$\underline{B}(s_k) \underline{u}_k = 0 \quad (2.9)$$

where

\underline{u}_k = n -dimensional, complex valued modal
vector

$\underline{B}(s_k)$ = system matrix evaluated at the pole
location $s = s_k$

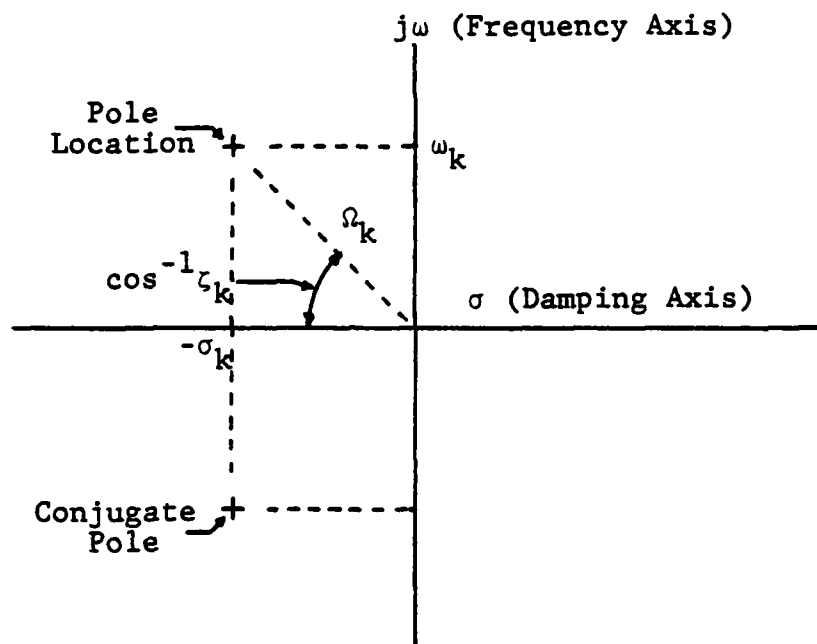


Figure 2.1. Poles of a Single Degree of Freedom System

Potter and Richardson (9) have shown that, when the modal vectors are defined as above, the residue matrices (\underline{A}_k) can be written as

$$\underline{A}_k = a_k \underline{u}_k \underline{u}_k^T \quad (2.10)$$

where

a_k = complex valued scalar
 $\underline{u}_k \underline{u}_k^T$ = an $n \times n$ complex valued, symmetric matrix

In other words, the residue matrix, \underline{A}_k , can be determined, to within a multiplicative constant (complex valued), by a mode shape vector \underline{u}_k , which is the solution to the homogeneous equation (2.9).

Using equation (2.10), the transfer matrix $\underline{H}(s)$ can now be written in the form

$$\underline{H}(s) = \sum_{k=1}^{2n} \frac{a_k \underline{u}_k \underline{u}_k^T}{s - s_k} \quad (2.11)$$

or it can be written as a summation of n -conjugate pairs

$$\underline{H}(s) = \sum_{k=1}^n \left[\frac{a_k \underline{u}_k \underline{u}_k^T}{s - s_k} + \frac{a_k^* \underline{u}_k^* \underline{u}_k^{*T}}{s - s_k^*} \right] \quad (2.12)$$

Equations (2.11) and (2.12) are the forms of the transfer function from which all the desired modal parameters (frequency, damping ratio, mode shape) can be extracted.

Potter and Richardson (9), and also (11),

have shown that because of the form of the \underline{A}_k matrix (as defined by equation (2.10)), only one row or column of the transfer matrix need be measured and analyzed, since all other rows and columns contain redundant information. For example, consider a two degree of freedom system with two sets of complex conjugate pairs of poles and modal vectors.

$$s_1, \underline{u}_1 = \begin{Bmatrix} u_{11} \\ u_{21} \end{Bmatrix} \quad s_1^*, \underline{u}_1^* = \begin{Bmatrix} u_{11}^* \\ u_{21}^* \end{Bmatrix}$$

$$s_2, \underline{u}_2 = \begin{Bmatrix} u_{12} \\ u_{22} \end{Bmatrix} \quad s_2^*, \underline{u}_2^* = \begin{Bmatrix} u_{12}^* \\ u_{22}^* \end{Bmatrix}$$

Expanding (2.12) for this case, the transfer matrix can be written as

$$\underline{H}(s) = a_1 \begin{bmatrix} \frac{u_{11}u_{11}}{s - s_1} & \frac{u_{11}u_{21}}{s - s_1} \\ \frac{u_{21}u_{11}}{s - s_1} & \frac{u_{21}u_{21}}{s - s_1} \end{bmatrix} + a_1^* \begin{bmatrix} \frac{u_{11}^*u_{11}^*}{s - s_1^*} & \frac{u_{11}^*u_{21}^*}{s - s_1^*} \\ \frac{u_{21}^*u_{11}^*}{s - s_1^*} & \frac{u_{21}^*u_{21}^*}{s - s_1^*} \end{bmatrix}$$

$$+ a_2 \begin{bmatrix} \frac{u_{12}u_{12}}{s - s_2} & \frac{u_{12}u_{22}}{s - s_2} \\ \frac{u_{22}u_{12}}{s - s_2} & \frac{u_{22}u_{22}}{s - s_2} \end{bmatrix} + a_2^* \begin{bmatrix} \frac{u_{12}^*u_{12}^*}{s - s_2} & \frac{u_{12}^*u_{22}^*}{s - s_2} \\ \frac{u_{22}^*u_{12}^*}{s - s_2} & \frac{u_{22}^*u_{22}^*}{s - s_2} \end{bmatrix} \quad (2.13)$$

Note that in each row and column, the numerators contain the same modal vector multiplied by a component of itself. The modal vectors and pole locations can be identified from any row or column of the transfer matrix except those which have components which are zero (node points).

In practice, the pole locations s_k and one row or column of the residue matrix \underline{A}_k are actually identified from one row or column of the measured transfer function data. Suppose that in the two degree of freedom case discussed above the first column of the residue matrix for the k^{th} mode (\underline{A}_k) is measured. This column can be expressed as

$$\underline{r}_1 = \begin{Bmatrix} a_1 u_{11} u_{11} \\ a_1 u_{11} u_{21} \end{Bmatrix} \quad (2.14)$$

If we perform the multiplication of $\underline{r}_1 \underline{r}_1^T$ we obtain

$$\underline{r}_1 \underline{r}_1^T = \begin{bmatrix} a_1^2 u_{11}^4 & a_1^2 u_{11}^3 u_{21} \\ a_1^2 u_{11}^3 u_{21} & a_1^2 u_{11}^2 u_{21}^2 \end{bmatrix} \quad (2.15)$$

Now if we scale equation (2.15) by dividing each element by $a_1 u_{11}^2$, we get

$$\frac{\underline{r}_1 \underline{r}_1^T}{a_1 u_{11}^2} = \begin{bmatrix} a_1 u_{11} u_{11} & a_1 u_{11} u_{21} \\ a_1 u_{11} u_{21} & a_1 u_{21} u_{21} \end{bmatrix} \quad (2.16)$$

which is the same as the first matrix in equation (2.13). In general, the entire k^{th} residue matrix can be found from the q^{th} row or column measured, say \underline{r}_q . Then

$$\underline{A} = \frac{\underline{r}_q \underline{r}_q^T}{r_{qq}} \quad (2.17)$$

where

\underline{A} = the residue matrix associated with the k^{th} pole

r_{qq} = the q^{th} component of the residue vector \underline{r}_q measured at the k^{th} pole. For single point excitation, r_{qq} is the residue of mode k measured at the driving point.

2.4 Complex Mode Shapes

The previous development of a structural dynamic model required that the damping matrix be symmetric and real valued. If we impose no further restrictions on the damping assumption, then the modal vectors will, in general, be complex valued. When the modal vectors are real valued, all points on the structure reach their minimum or maximum values simultaneously. This is not the case if the modal vectors are complex. Recall from equation (2.8) that the component of the transfer matrix for a single mode k can be written

$$\underline{H}_k(s) = \frac{\underline{A}_k}{s - s_k} + \frac{\underline{A}_k^*}{s - s_k^*} \quad (2.18)$$

For each complex conjugate pair of poles there is a corresponding complex conjugate pair of modal vectors. The ij^{th} element of $\underline{H}_k(s)$ is (after dropping the ij subscripts)

$$h_k(s) = \frac{v_k}{s - s_k} + \frac{v_k^*}{s - s_k^*} \quad (2.19)$$

where

$v_k = a_k u_{ki} u_{kj}$, the complex residue of mode k

from the ij^{th} frequency response.

The inverse Laplace transform of equation (2.19) is the impulse response of mode k for point i in the structure with input at point j . If only mode k could be excited by a unit impulse, the time domain response would be

$$\begin{aligned} x_k(t) &= v_k \exp(s_k t) \\ &+ v_k^* \exp(s_k^* t) \\ &= 2 \exp(-\sigma_k t) \left[\text{Re}(v_k) \cos \omega_k t \right. \\ &\quad \left. - \text{Im}(v_k) \sin \omega_k t \right] \\ &= 2 \exp(-\sigma_k t) \left| v_k \right| \cos(\omega_k t + \alpha_k) \end{aligned}$$

where

$$2 \left| v_k \right| = \text{peak amplitude of the impulse response} \\ \text{(twice the magnitude of the complex residue)}$$

$$\alpha_k = \arctan \frac{\text{Im}(v_k)}{\text{Re}(v_k)}, \text{ which is the phase} \\ \text{angle of the complex residue}$$

Notice that when $\alpha_k = 0$ or 180° the residue vector is real valued. It is this phase angle which determines the phase of the complex mode vector. If there were no damping in the system the mode vectors are real

valued and all points on the structure reach their minimum or maximum displacement simultaneously, i.e., α_k is 0° or 180° . When α_k is an angle other than 0° or 180° then the node lines (lines of zero displacement) will not be stationary as in the undamped case. It is this phase angle that is neglected in some modal parameter estimation techniques. In the techniques described in this thesis, this phase angle is accounted for and does not present major problems

2.5 Deriving Mass, Stiffness, and Damping Matrices From Frequency Response Data

In (9), Potter and Richardson have shown that the mass, stiffness, and damping matrices (\underline{M} , \underline{K} , and \underline{C}), and hence the system matrix \underline{B} , can readily be reconstructed from the measured modal vectors. The summation in equation (2.11) can be written as

$$\underline{H}(s) = \underline{\theta} \underline{\Lambda}^{-1} \underline{\theta}^T \quad (2.10)$$

which is an $n \times n$ matrix where the columns of $\underline{\theta}$ comprise the \underline{u}_k modal vectors

$$\underline{\theta} = \begin{bmatrix} \frac{\underline{u}_1}{\sqrt{\underline{u}_1^T \underline{u}_1}} & \frac{\underline{u}_2}{\sqrt{\underline{u}_2^T \underline{u}_2}} & \frac{\underline{u}_3}{\sqrt{\underline{u}_3^T \underline{u}_3}} & \dots & \frac{\underline{u}_n}{\sqrt{\underline{u}_n^T \underline{u}_n}} \\ \vdots & \vdots & \vdots & \dots & \vdots \end{bmatrix} \quad (n \times 2n)$$

and $\underline{\Lambda}^{-1}$ is a diagonal matrix containing all of the s dependence.

$$\underline{\Lambda}^{-1} = \begin{bmatrix} \frac{a_1}{s - s_1} & & & \underline{0} \\ & \ddots & & \\ & & & \\ \underline{0} & & & \frac{a_{2n}}{s - s_{2n}} \end{bmatrix} \quad (2n \times 2n)$$

Recall from equation (2.4) that

$$\underline{B}(s) = \underline{M}s^2 + \underline{C}s + \underline{K}$$

and evaluate $\underline{B}(s)$ at $s = 0$, then

$$\underline{K} = \underline{B}(0) = \underline{H}(0)^{-1}$$

One can see that $\underline{H}(0)$ can be obtained by setting $s = 0$ in $\underline{\Lambda}^{-1}$

$$\underline{K} = \underline{H}(0)^{-1} = (\underline{\theta} \underline{\Lambda}(0)^{-1} \underline{\theta}^T)^{-1} \quad (2.21)$$

Thus the stiffness matrix can be derived from the measured modal vectors \underline{u}_k and the identified a_k and s_k complex scalars.

Recall also that since \underline{H} equals \underline{B}^{-1} ,

$$\underline{H} \underline{B} = \underline{I} \quad (2.22)$$

Differentiating (2.22) with respect to s gives

$$\underline{H} \underline{B}' + \underline{H}' \underline{B} = 0 \quad (2.23)$$

and differentiating a second time gives

$$\underline{H} \underline{B}'' + 2 \underline{H}' \underline{B}' + \underline{H}'' \underline{B} = 0 \quad (2.24)$$

where the prime denotes differentiation with respect to s . If we then differentiate equation (2.4) with respect to s we obtain

$$\underline{B}' = 2 \underline{M} s + \underline{C} \quad (2.25)$$

which when evaluated at $s = 0$ yields the damping matrix.

$$\underline{C} = \underline{B}'(0) \quad (2.26)$$

Rearranging equation (2.23) gives

$$\underline{B}' = -\underline{H}^{-1} \underline{H}' \underline{B}$$

or

$$\underline{B}' = -\underline{B} \underline{H}' \underline{B}$$

which when evaluated at $s = 0$ yields the damping matrix.

$$\underline{C} = -\underline{B}(0) \underline{H}'(0) \underline{B}(0) = -\underline{K} \underline{H}'(0) \underline{K}$$

or

$$\underline{C} = -\underline{K} \left[\underline{\theta} (\underline{\Lambda}^{-1})' (0) \underline{\theta}^T \right] \underline{K} \quad (2.27)$$

Differentiating equation (2.25) with respect to s gives

$$\underline{M} = \frac{1}{2} \underline{B}'' \quad (2.28)$$

Rearranging equation (2.24) yields

$$\underline{B}'' = -2 \underline{H}^{-1} \underline{H}' \underline{B}' - \underline{H}^{-1} \underline{H}'' \underline{B} \quad (2.29)$$

Using the relation $\underline{B} = \underline{H}^{-1}$ and evaluating \underline{B}'' at $s = 0$

gives

$$\begin{aligned}\underline{M} &= -\underline{B}(0)\underline{H}'(0)\underline{B}'(0) - \frac{1}{2}\underline{B}(0)\underline{H}''(0)\underline{B}(0) \\ &= -\underline{K}\underline{H}'(0)\underline{C} - \frac{1}{2}\underline{K}\underline{H}''(0)\underline{K}\end{aligned}$$

or

$$\underline{M} = -\underline{K} \begin{bmatrix} \underline{\theta}(\underline{\Lambda}^{-1})'(0)\underline{\theta}^T \\ -\frac{1}{2}\underline{K} \begin{bmatrix} \underline{\theta}(\underline{\Lambda}^{-1})''(0)\underline{\theta}^T \end{bmatrix} \underline{K} \end{bmatrix} \underline{C} \quad (2.30)$$

Thus by defining the matrices

$$\underline{\Lambda}^{-1}(0) = \begin{bmatrix} -\frac{a_1}{s_1} & 0 \\ 0 & -\frac{a_{2n}}{s_{2n}} \end{bmatrix}$$

$$(\underline{\Lambda}^{-1})'(0) = \begin{bmatrix} -\frac{a_1}{s_1^2} & 0 \\ 0 & -\frac{a_{2n}}{s_1^2} \end{bmatrix}$$

$$(\underline{A}^{-1})''(0) = \begin{bmatrix} -\frac{2a_1}{s_1^3} & \underline{0} \\ & \ddots \\ \underline{0} & -\frac{2a_{2n}}{s_{2n}^3} \end{bmatrix}$$

the mass, stiffness and damping matrices for the measured system can be obtained from the poles s_k , scalars a_k , and modal vectors u_k which are determined from the experimental frequency response functions.

2.6 Summary

In summary then it has been shown that if the transfer matrix of a structure can be measured (in the Laplace domain) then all of the modes of vibration of the structure can be characterized, and a matrix model developed for analysis. The problem that remains is to measure the transfer function. Since the frequency response of a structure is the transfer function evaluated along the $j\omega$ axis, it then contains the necessary information required to

model the transfer function (or matrix). In practice then, the frequency response functions are measured and then curve fitting is performed on the data to curve fit into the s-plane transfer matrix. Chapter III will discuss some of the different curve fitting methods.

CHAPTER III

MODAL PARAMETER ESTIMATION TECHNIQUES

3.1 Parameter Identification

When a linear structure is excited by a broad band input many of its modes of vibration are excited simultaneously. Therefore, because of the linearity, the transfer functions are really the sums of the resonance curves for each of the modes of vibration (see figure 3.1).

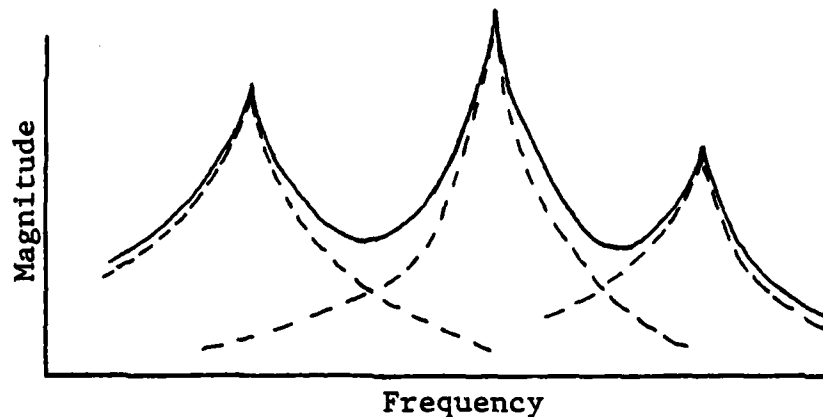


Figure 3.1. Multi Degree of Freedom Transfer Function

At any given frequency, the transfer function represents the sum of the motion of all the modes of vi-

bration which have been excited. The dashed lines in Figure 3.1 represent a number of single degree of freedom modes which when added together form the multi degree of freedom transfer function. The degree of overlap (modal overlap) is governed by the amount of damping of the modes and their frequency separation. This modal overlap is caused by the contribution of the tails of adjacent modal peaks. Figure 3.2 shows a transfer function which is lightly damped and has sufficient frequency separation so that there is little modal overlap.

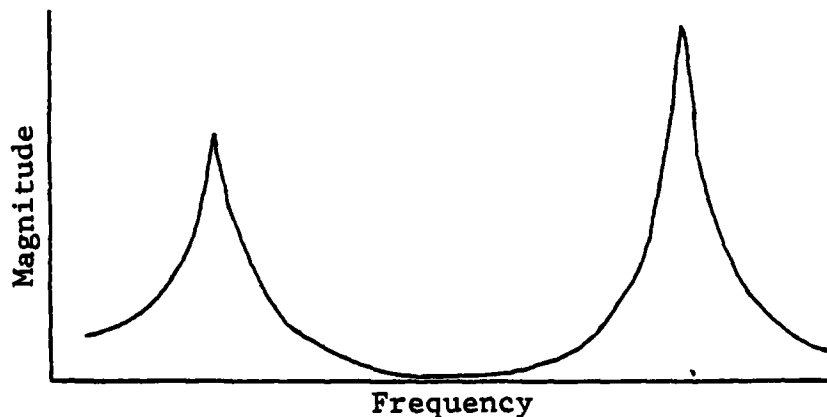


Figure 3.2. Light Modal Overlap

Figure 3.3 illustrates modes with heavy damping and very little frequency separation. If the damping is

light and the peaks of the response are sufficiently

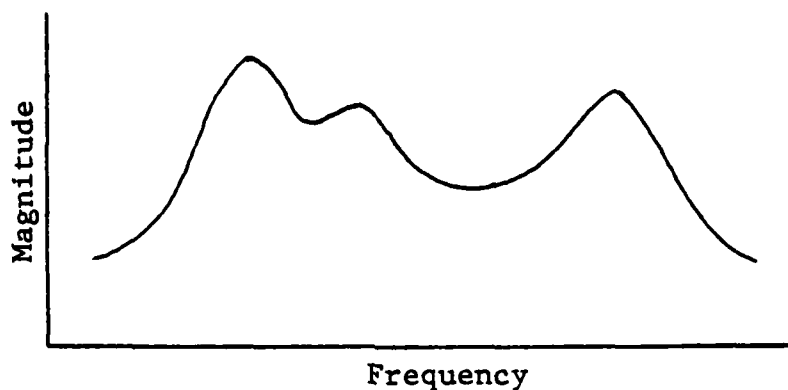


Figure 3.3. Heavy Modal Overlap

separated, then the response data in the vicinity of each peak can be treated as if it were a single degree of freedom system. However, if the modal overlap is heavy, i.e., the "tails" of adjacent modes contribute significantly to the magnitude of the mode being investigated, then a single degree of freedom approach will not work. For these cases, the parameters of the modes must be estimated simultaneously through a multi degree of freedom approach.

Once the natural frequencies, damping ratios, and mode shapes are determined, an analytical expression for the Laplace domain transfer function can be determined. Once the analytical expression is ob-

tained, it can be used to predict the response of the system to a particular type of input.

3.2 Single Degree of Freedom Techniques

If the frequency response data exhibits light damping and the peaks are separated sufficiently so that very little modal overlap is present then the following techniques may be considered.

3.2.1 Quadrature Response Technique

Recall that the transfer function of a linear system for a single mode k can be written as

$$h_k(s) = \frac{a_k}{s - s_k} + \frac{a_k^*}{s - s_k^*} \quad (3.1)$$

where the a_k is the complex residue at the k^{th} pole.

If we let $s = j\omega$, the frequency response function can be written

$$\begin{aligned} h_k(j\omega) &= \frac{a_k}{j\omega - s_k} + \frac{a_k^*}{j\omega - s_k^*} \\ &= \frac{a_k}{j\omega + \sigma_k - j\omega_k} + \frac{a_k^*}{j\omega + \sigma_k + j\omega_k} \end{aligned} \quad (3.2)$$

The magnitude of a typical frequency response function is shown below in figure 3.4.

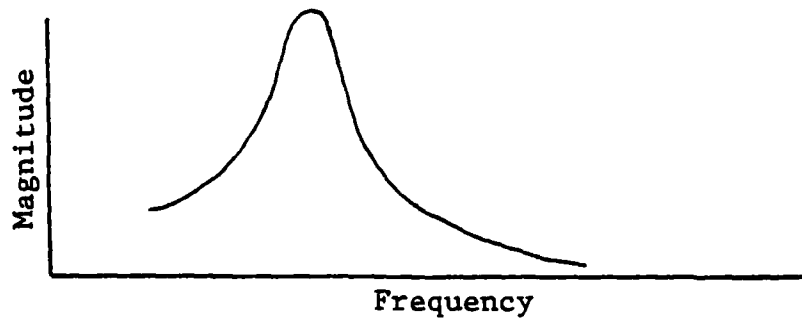


Figure 3.4. Frequency Response Curve For A Single Degree Of Freedom

In the neighborhood of $\omega \approx \omega_k$, the majority of the resonance curve can be approximated by

$$h_k(j\omega) \approx \frac{a_k}{j\omega - s_k} \quad (3.3)$$

If, for convenience, we remove a factor of $\frac{1}{2j}$ from the residue, then equation (3.3) can be written

$$h_k(j\omega) \approx \frac{r_k}{2j(j\omega - s_k)} = \frac{r_k}{2((\omega_k - \omega) + j\sigma_k)} \quad (3.4)$$

which can be written in real and imaginary parts

$$\text{Real} [h_k(j\omega)] = \frac{1}{2} \left[\frac{r_1(\omega_k - \omega) + r_2\sigma_k}{(\omega_k - \omega)^2 + \sigma_k^2} \right]$$

$$\text{Imag} \left[h_k(j\omega) \right] = \frac{1}{2} \left[\frac{r2_k(\omega_k - \omega) - r1_k\sigma_k}{(\omega_k - \omega)^2 + \sigma_k^2} \right] \quad (3.5)$$

where

$$r_k = \frac{a_k}{2j} = r1_k + jr2_k$$

$$s_k = -\sigma_k + j\omega_k$$

When $\omega = \omega_k$ the above expressions become

$$\text{Real} \left[h_k(j\omega) \right] = \frac{r2_k}{2\sigma_k}$$

$$\text{Imag} \left[h_k(j\omega) \right] = -\frac{r1_k}{2\sigma_k} \quad (3.6)$$

In cases of light damping (or proportional damping) the residues, r_k , are nearly (exactly for proportional damping) real valued, i.e., $r2_k \approx 0$. When this assumption is valid then the natural frequency and mode shape data can be extracted from the quadrature, or imaginary part, of $h_k(j\omega)$. The natural frequency is the frequency at which the peak in the quadrature response occurs, or the frequency where the coincident (real) part of $h_k(j\omega)$ is zero. The mode shape contribution is simply the magnitude of the quadrature

response at the resonant frequency. The damping ratio can be determined by the familiar half-power (bandwidth) method, i.e.,

$$\zeta \approx \frac{1}{2} \left[\frac{\omega_2 - \omega_1}{\omega_n} \right] \quad (3.7)$$

where ω_1 , and ω_2 are the frequencies at which the response is reduced to $\frac{1}{\sqrt{2}}$ times the peak value, and ω_n is the natural frequency. As stated before, this method is only good for cases where the damping is very light. One can also get into problems with this method if the modes are closely spaced in frequency and there is significant influence on each mode due to adjacent peaks. Because of the limitations of this method it will not be discussed further in this thesis.

3.2.2 Method of Kennedy and Pancu

In 1947, Charles Kennedy and C. D. P. Pancu, published a paper entitled, "Use of Vectors in Vibration Measurement and Analysis" (6). This paper set the stage for the present day techniques used in modal analysis. The main purpose of their paper was to identify the normal modes of vibration of mechanical sys-

tems. They assumed that the damping in the system was proportional to the displacement and 90° out of phase with it. They also assumed that the off-resonant vibration is constant in phase and magnitude as the system passed through a resonance. The authors made use of a vector response plot, more commonly called a polar plot or Nyquist plot, which plotted both real and imaginary components of the frequency response data vs. frequency. An example of a Nyquist plot is illustrated in Figure 3.5. Their basis for using this type of plot was that near a resonant frequency, the polar plot would describe a circular arc. The plot for a single degree of freedom system is shown in Figure 3.6. In terms of the analytical transfer function,

$$h_k(\omega) = \frac{|r_k| e^{j\alpha_k t}}{(\omega_k - \omega) + j\sigma_k} \quad (3.8)$$

where

$$|r_k| = \left| \frac{a_k}{2} \right|, \text{ magnitude of the complex residue}$$

$$\alpha_k = \text{phase angle of the residue}$$

If $|r_k| = 1$ and $\alpha_k = 0$ then it can be shown that

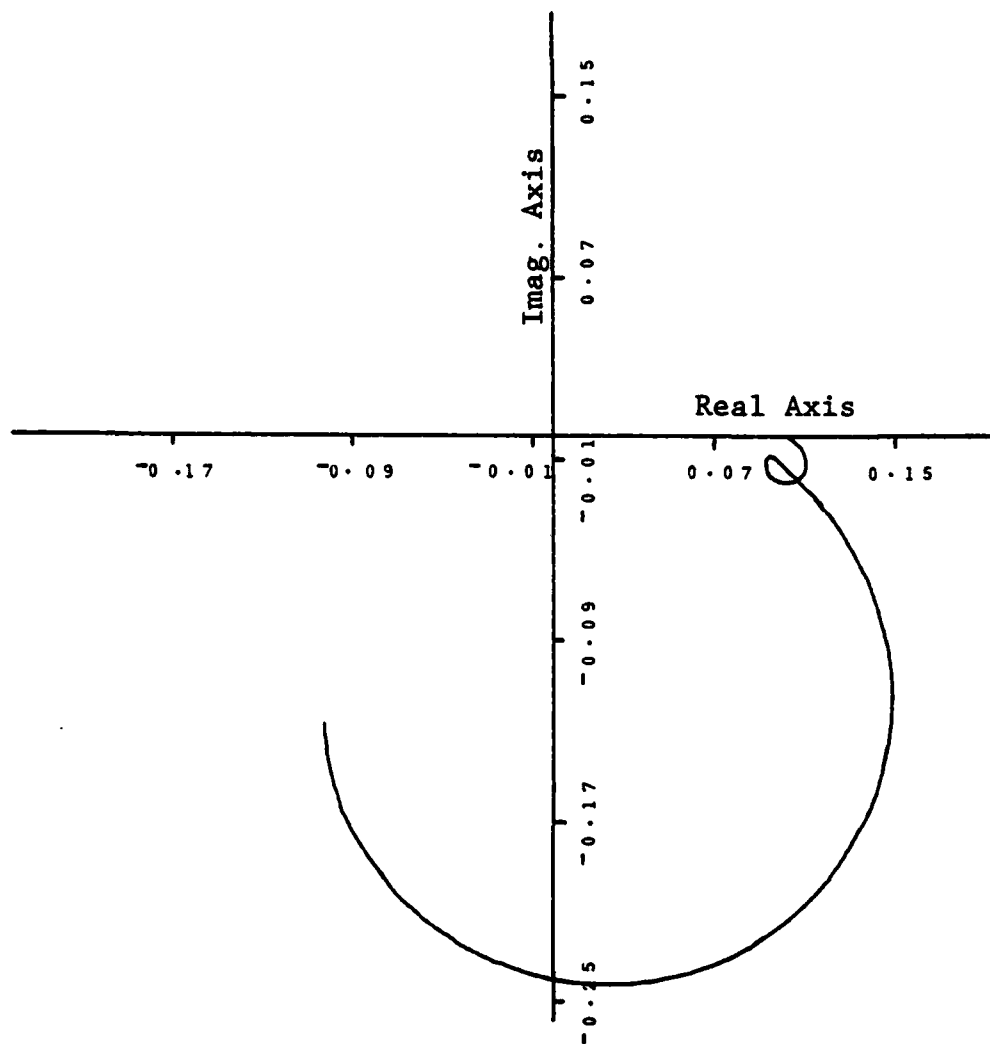


Figure 3.5. Polar Plot Of A Frequency Response Function

$$\operatorname{Re} [H_k]^2 + (\operatorname{Im} [H_k] + \frac{1}{4\sigma_k})^2 = \frac{1}{16\sigma_k^2} \quad (3.9)$$

which is a circle in the Nyquist plane with a radius of $\frac{1}{4\sigma_k}$ and centered at $-j(\frac{1}{4\sigma_k})$. The complex residue

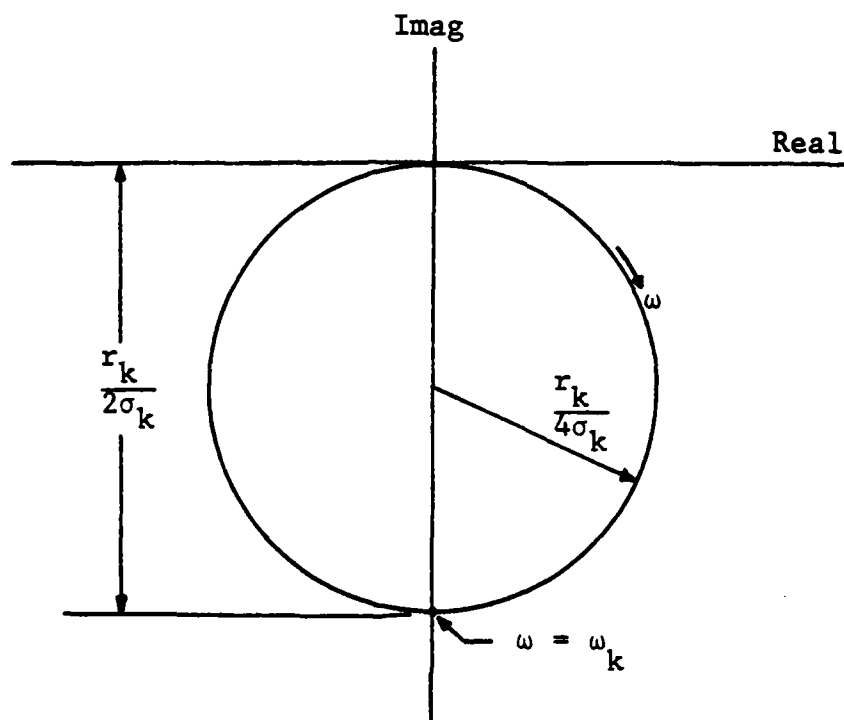


Figure 3.6. Modal Resonance In Nyquist Plane

vector, r_k , merely expands the radius of the circle and rotates it in the Nyquist plane clockwise by an angle α_k away from the negative imaginary axis (see

Figure 3.7). Kennedy and Pancu only considered the

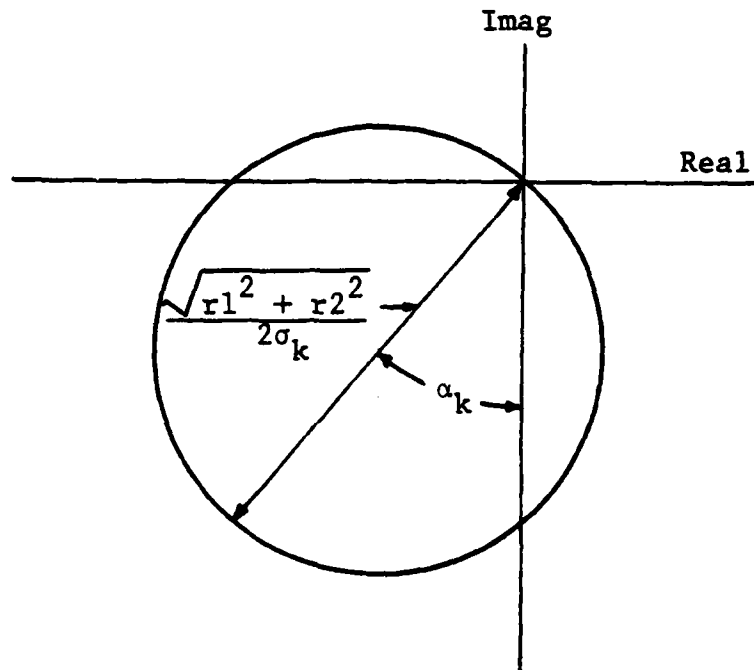


Figure 3.7. Complex Modal Resonance
In Nyquist Plane

cases where the residue vector was real valued, i.e.,

$$\alpha_k = 0.$$

It was shown by Kennedy and Pancu that the natural frequency(s) of a system could be determined from a Nyquist Plot by observing where the arc length of the plot was a maximum for a given change in fre-

quency (see Figure 3.8). The arc length will increase

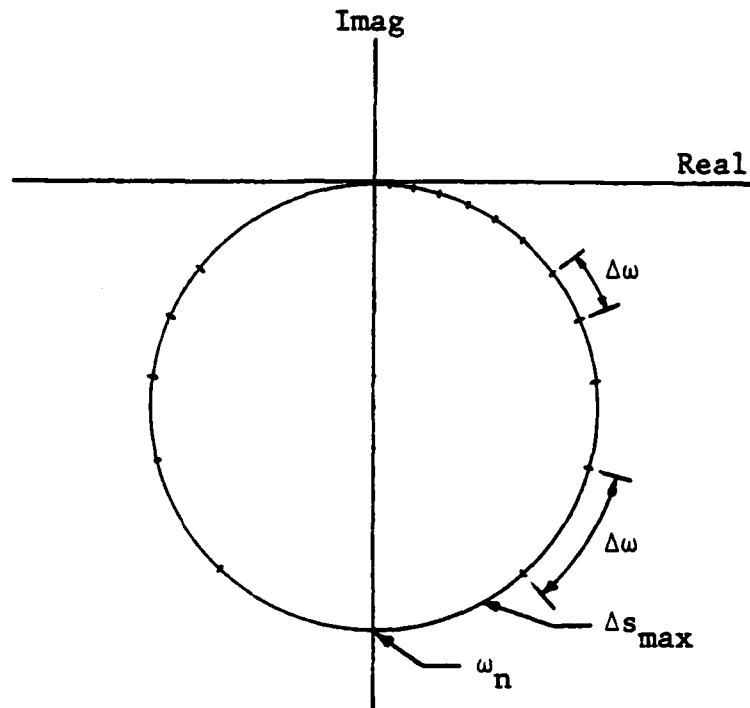


Figure 3.8. Determination of Natural Frequency From Nyquist Plot

until ω passes through a resonant frequency, then the length will decrease and later will increase again as another resonant frequency is approached. The resonant frequencies can be determined by picking off the points where the arc length reaches a local maximum.

Once the natural frequencies are found, use

is made of the fact that near a resonance the arc approximately describes a circle. A circle is then fit to the data near each resonant frequency.

One method that can be used to circle fit the data is the method of least squares. The general equation of a circle is

$$x^2 + y^2 + ax + by + c = 0 \quad (3.10)$$

where a, b, and c are constants related to the location of the center of the circle and the radius.

$$x_{\text{center}} = -\frac{1}{2}a$$

$$y_{\text{center}} = -\frac{1}{2}b$$

$$\text{radius} = \left[\left(\frac{a}{2}\right)^2 + \left(\frac{b}{2}\right)^2 - c \right]^{\frac{1}{2}}$$

For the purpose of relating these equations to the Nyquist Plane, define

$$x = \text{Real} \left[H_k \right]$$

$$y = \text{Imag} \left[H_k \right]$$

Now define the error function to be equal to

$$e = x^2 + y^2 + ax + by + c \quad (3.11)$$

Squaring this error and summing this result over all the discrete frequency points in the area of the desired fit gives

$$\sum_{k=1}^n e^2 = \sum_{k=1}^n (x^2 + y^2 + ax + by + c)^2 \quad (3.12)$$

To minimize the error squared, the partial derivatives of (3.12) with respect to a , b , and c should equal zero. Thus we have

$$\begin{aligned} 2 \sum_{k=1}^n (x^2 + y^2 + ax + by + c)x &= 0 \\ 2 \sum_{k=1}^n (x^2 + y^2 + ax + by + c)y &= 0 \quad (3.13) \\ 2 \sum_{k=1}^n (x^2 + y^2 + ax + by + c) &= 0 \end{aligned}$$

In matrix form we get equations (3.14). Using Gaussian elimination, the constants a , b , and c can be found which then will give the location of the center of the circle and its radius. Once the circle

is determined it can be treated as a single degree of

$$\begin{bmatrix} \sum_{k=1}^n x^2 & \sum_{k=1}^n xy & \sum_{k=1}^n x \\ \sum_{k=1}^n xy & \sum_{k=1}^n y^2 & \sum_{k=1}^n y \\ \sum_{k=1}^n x & \sum_{k=1}^n y & n \end{bmatrix} \begin{bmatrix} a \\ b \\ c \end{bmatrix} = \begin{bmatrix} -\sum_{k=1}^n (x^3 + xy^2) \\ -\sum_{k=1}^n (x^2y + y^3) \\ -\sum_{k=1}^n (x^2 + y^2) \end{bmatrix} \quad (3.14)$$

freedom system where the diameter of the circle can be used as the magnitude of a component of the mode shape and the phase angle can be computed knowing the location of the center. Consider the circle shown in Figure 3.9. The coordinates of the center of the circle are now known. Also, the coordinates of the point where ω equals the natural frequency are known. The angle α_k can then be determined from the following relation

$$\alpha_k = \arctan \frac{|x - x_c|}{|y - y_c|} \quad (3.15)$$

where

x_c = Real axis coordinate of the circle center

y_c = Imaginary axis coordinate of the circle center
center

The sign of the angle can be determined from the direction of rotation from the imaginary axis. A positive angle is rotated clockwise from the $j\omega$ axis.

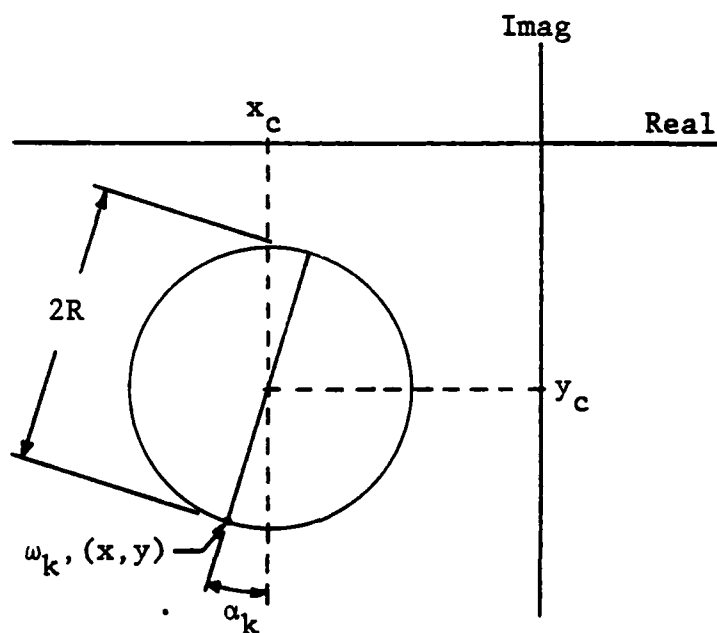


Figure 3.9. Circle Coordinated

The damping ratio can be determined in different ways. One way provides for the ratio to be

calculated at two different points and then averaged.
 Consider the equation of motion in the Laplace domain
 of a single degree of freedom system

$$(ms^2 + cs + k)X(s) = F(s) \quad (3.16)$$

The transfer function can be written

$$\begin{aligned} \frac{X(s)}{F(s)} &= \frac{1}{m(s^2 + 2\zeta\omega_n s + \omega_n^2)} \\ &= \frac{(1/k)\omega_n^2}{s^2 + 2\zeta\omega_n s + \omega_n^2} \end{aligned}$$

or

$$\frac{X(s)}{X(s)_{sta}} = \frac{\omega_n^2}{s^2 + 2\zeta\omega_n s + \omega_n^2} \quad (3.17)$$

where

$$2\zeta\omega_n = c/m$$

$$\omega_n^2 = k/m$$

$$X(s)_{sta} = F(s)/k = \text{"static displacement"}$$

Then

$$H(j\omega) = \frac{X(j\omega)}{X(j\omega)_{sta}} = \frac{\omega_n^2}{(\omega_n^2 - \omega^2) + j2\zeta\omega\omega_n}$$

$$= \frac{\omega_n^2}{(\omega_n^2 - \omega^2)^2 + (2\zeta\omega\omega_n)^2} e^{-j\phi} \quad (3.18)$$

where

$$\phi = \arctan \frac{2\zeta\omega\omega_n}{\omega_n^2 - \omega^2} \quad (3.19)$$

Looking at the Nyquist plot for this function, Figure 3.10, one can see the phase angle ϕ for an arbitrary ω .

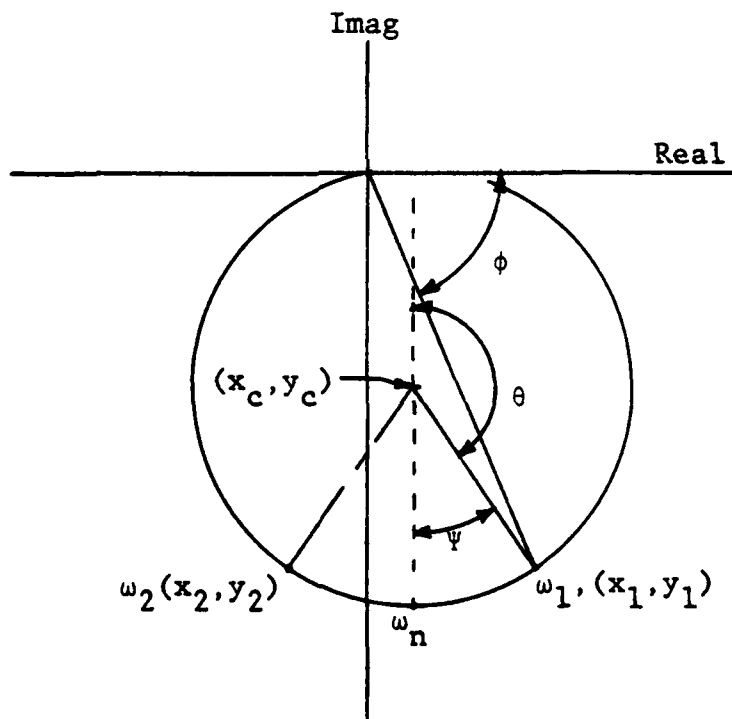


Figure 3.10. Nyquist Plot Of Single Degree Of Freedom System

Now define $\theta = 2\phi$ where θ is measured from the diameter of the circle drawn through the resonant frequency. Substituting $\theta = 2\phi$ into equation (3.19) and solving for ζ gives

$$\zeta = \frac{(\omega_n^2 - \omega^2) \tan(\theta/2)}{2\omega\omega_n} \quad (3.20)$$

The only information needed to get the angle θ are the coordinates of the center of the circle and the coordinates of a frequency point on one side or the other of the resonant frequency. Consider the example shown in Figure 3.10.

$$\psi = \arctan \frac{|x_1 - x_c|}{|y_1 - y_c|}$$

$$\theta = 180^\circ - \psi$$

Substituting into equation (3.20) gives

$$\zeta = \frac{(\omega_n^2 - \omega_1^2) \tan \frac{180 - \psi}{2}}{2\omega_1\omega_n}$$

The same thing can be done using ω_2 and then the two values of ζ averaged.

This method of circle fitting is accomplished for each resonant frequency observed in the Nyquist

plot for a given frequency response. If this is accomplished for each frequency response in one row or column of the transfer matrix, then the mode shapes can be determined, i.e.

$$\text{Mode 1} = \left\{ \begin{array}{l} (a_1)_{11} \quad \angle (\alpha_1)_{11} \\ (a_1)_{21} \quad \angle (\alpha_1)_{21} \end{array} \right\}$$

where

$(a_1)_{11}$ = diameter of circle at ω_1 determined from frequency response h_{11}

$(a_1)_{21}$ = diameter of circle at ω_1 determined from frequency response h_{21}

and similarly for the phase angles $(\alpha_k)_{ij}$.

Immediately one can see a problem with this type of approach. If the modes happen to be closely coupled where one mode dominates, the circle fit of the smaller mode may not have sufficient points to resolve the amplitude of the residue, i.e., the diameter of the circle fit through the smaller mode may be incorrect thus giving rise to errors in the mode shape and also the damping ratio associated with that mode.

In order to reduce the limitations imposed by single degree of freedom assumptions, one must consider a multi-degree of freedom curve fit, which is the subject of Section 3.3.

Chapter IV will present example problems using this method of determining modal parameters. Also, Appendix A gives a listing of a computer algorithm derived for circle fitting frequency response data.

3.3 Multi Degree of Freedom Curve Fitting

For cases where the amount of modal overlap is sufficient to cause significant errors by use of single degree of freedom techniques, a multi degree of freedom technique must be used. Two techniques will be described in this section.

3.3.1 Complex Curve Fit

This technique is one which matches the summation

$$h(s) = \sum_{k=1}^n \left[\frac{a_k}{s - s_k} + \frac{a_k^*}{s - s_k^*} \right] \quad (3.21)$$

along the frequency axis ($s = j\omega$) to the measured frequency response function data. A least squares error estimation is used to account for modes that are outside of the frequency range of interest.

Consider equation (3.21) evaluated at $s = j\omega$.

$$h(j\omega) = \sum_{k=1}^n \frac{a_k}{j\omega - s_k} + \frac{a_k^*}{j\omega - s_k^*} \quad (3.22)$$

This summation is over n -modes. The summation can be rewritten as

$$h(j\omega) = \frac{a_m}{j\omega - s_m} + \frac{a_m^*}{j\omega - s_m^*} + \sum_{\substack{k=1 \\ k \neq m}}^n \frac{a_k}{j\omega - s_k} + \frac{a_k^*}{j\omega - s_k^*} \quad (3.23)$$

If we define

$$R_m = \frac{a_m^*}{j\omega - s_m^*} + \sum_{\substack{k=1 \\ k \neq m}}^n \frac{a_k}{j\omega - s_k} + \frac{a_k^*}{j\omega - s_k^*} \quad (3.24)$$

then equation (3.23) can be written

$$\begin{aligned} h(j\omega) &= \frac{a_m}{j\omega - s_m} + R_m \\ &= \frac{a_m}{\sigma_m + j(\omega - \omega_m)} + R_m \end{aligned} \quad (3.25)$$

If the system is lightly damped, i.e., σ_m is small, it is noted that in the neighborhood of $\omega = \omega_m$, the first term in equation (3.25) dominates, and R_m is nearly constant for small changes in ω . Using this assumption, consider the m^{th} peak in the magnitude curve of $h(j\omega)$ (see Figure 3.11). Pick two points on the curve, one on each side of the peak. Now then, evaluate

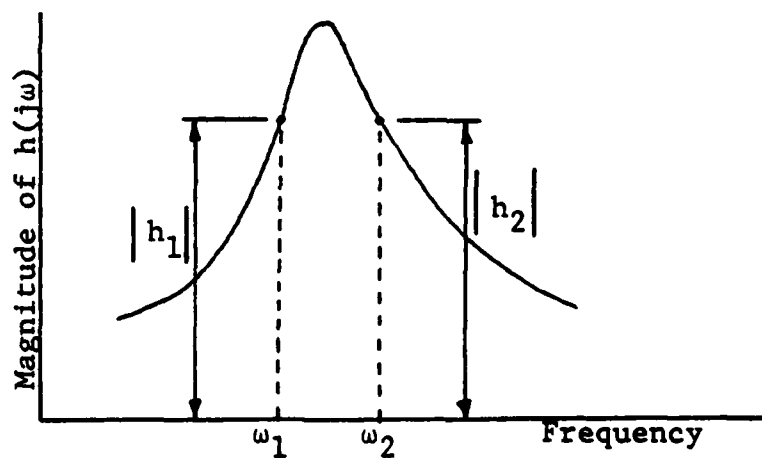


Figure 3.11. Two Point Estimation

equation (3.25) at each of the two points to get

$$h_1 = h(j\omega_1) = \frac{a_m}{j\omega_1 - s_m} + R_m \quad (3.26)$$

$$h_2 = h(j\omega_2) = \frac{a_m}{j\omega_2 - s_m} + R_m \quad (3.27)$$

Solving for a_m results in

$$\begin{aligned} a_m &= (h_1 - R_m)(j\omega_1 - s_m) \\ &= (h_2 - R_m)(j\omega_2 - s_m) \end{aligned} \quad (3.28)$$

which after averaging yields

$$\begin{aligned} a_m &= \frac{1}{2} \left[(h_1 - R_m)(j\omega_1 - s_m) \right. \\ &\quad \left. + (h_2 - R_m)(j\omega_2 - s_m) \right] \end{aligned} \quad (3.29)$$

Also, s_m can be determined from equation (3.28)

$$s_m = \frac{j\omega_1(h_1 - R_m) - j\omega_2(h_2 - R_m)}{h_1 - h_2} \quad (3.30)$$

Since these equations contain complex variables we can separate them into real and imaginary parts. For convenience in evaluation, define the following:

$$\begin{aligned} a_m &= a_m^r + ja_m^i \\ s_m &= -\sigma_m + j\omega_m \end{aligned}$$

$$\begin{aligned}
 R_m &= R_m^r + jR_m^i \\
 h_1 &= h_1^r + jh_1^i \\
 h_2 &= h_2^r + jh_2^i
 \end{aligned}
 \tag{3.31}$$

Substituting these relationships into equations (3.29) and (3.30) results in:

$$\begin{aligned}
 a_m^r + ja_m^i &= \frac{1}{2} \left[(h_1^r + jh_1^i - R_m^r - jR_m^i)(j\omega_1 + \sigma_m - j\omega_m) \right. \\
 &\quad \left. + (h_2^r + jh_2^i - R_m^r - jR_m^i)(j\omega_2 + \sigma_m - j\omega_m) \right]
 \end{aligned}
 \tag{3.32}$$

$$\begin{aligned}
 -\sigma_m + j\omega_m &= \frac{j\omega_1(h_1^r + jh_1^i - R_m^r - jR_m^i)}{h_1^r + jh_1^i - h_2^r - jh_2^i} \\
 &\quad - \frac{j\omega_2(h_2^r + jh_2^i - R_m^r - jR_m^i)}{h_1^r + jh_1^i - h_2^r - jh_2^i}
 \end{aligned}
 \tag{3.33}$$

Carrying out the indicated multiplications and divisions, and then separating into real and imaginary parts results in:

$$\sigma_m = \frac{-(\omega_2 - \omega_1)}{(h_1^r - h_2^r)^2 + (h_1^i - h_2^i)^2} \times$$

$$\begin{aligned} & \left[R_m^r (h_1^i - h_2^i) - R_m^i (h_1^r - h_2^r) \right. \\ & \left. + h_1^r h_2^i - h_1^i h_2^r \right] \end{aligned} \quad (3.34)$$

$$\begin{aligned} \omega_m &= \frac{1}{(h_1^r - h_2^r)^2 + (h_1^i - h_2^i)^2} \times \\ & \left\{ (\omega_2 - \omega_1) \left[R_m^r (h_1^r - h_2^r) + R_m^i (h_1^i - h_2^i) \right] \right. \\ & + \omega_1 \left[(h_1^r)^2 - h_1^r h_2^r + (h_2^r)^2 \right] \\ & \left. + \omega_2 \left[(h_1^i)^2 - h_1^i h_2^i + (h_2^i)^2 \right] \right\} \end{aligned} \quad (3.35)$$

$$\begin{aligned} a_m^r &= \frac{1}{2} \left[\sigma_m (h_1^r + h_2^r - 2R_m^r) \right. \\ & + \omega_m (h_1^i + h_2^i - 2R_m^i) - \omega_1 (h_1^i - R_m^i) \\ & \left. - \omega_2 (h_2^i - R_m^i) \right] \end{aligned} \quad (3.36)$$

$$\begin{aligned} a_m^i &= \frac{1}{2} \left[\sigma_m (h_1^i + h_2^i - 2R_m^i) \right. \\ & - \omega_m (h_1^r + h_2^r - 2R_m^r) + \omega_1 (h_1^r - R_m^r) \\ & \left. + \omega_2 (h_2^r - R_m^r) \right] \end{aligned} \quad (3.37)$$

From equations (3.34) through (3.37) it can be seen that s_m and a_m can be found if R_m is known. Recall that R_m is the contribution of the off-resonant terms

(equation (3.24)). If an estimate is made for R_m then values for s_m and a_m could be obtained and then an iterative technique could be established to improve the estimates.

The technique used in this paper is to assume R_m is initially zero and then solve for s_m and a_m . Then using these values, substitute into equation (3.24) and solve for a new R_m . This technique works fine when all of the modes are present in the frequency range of analysis and modal overlap is light. However, in real structures there are an infinite number of modes, all of which cannot be measured. Therefore it may be necessary to consider a contribution to the transfer functions due to modes with natural frequencies outside of the frequency range of analysis. This contribution can be considered either to be a complex constant or a complex function of frequency. For the purpose of simplicity, we will consider only the case where it is a complex constant.

The constant can be determined by a least squares fit to the following:

$$h(j\omega) = \sum_{k=1}^n \frac{a_k}{j\omega - s_k} + \frac{a_k^*}{j\omega - s_k^*} \quad (3.38)$$

where the summation includes only those modes in the frequency range of analysis. Define now the error function:

$$e = h(j\omega) - \sum_{k=1}^n \frac{a_k}{j\omega - s_k} + \frac{a_k^*}{j\omega - s_k^*} - R' \quad (3.39)$$

where R' is the complex least squares residual. Then the sum of the error squared becomes:

$$\sum_{i=1}^{k/2} e^2 = \sum_{i=1}^{k/2} \left[h_i - \sum_{k=1}^n \frac{a_k}{j(i\omega_0) - s_k} + \frac{a_k^*}{j(i\omega_0) - s_k^*} - R' \right]^2 \quad (3.40)$$

where

k = block size of the frequency response

ω_0 = frequency resolution = $2\pi\Delta f$

To minimize the least squares residual the following must be true:

$$R' = \sum_{i=1}^{k/2} \left\{ h_i \sum_{k=1}^n \left[\frac{a_k}{j(i\omega_0) - s_k} + \frac{a_k^*}{j(i\omega_0) - s_k^*} \right] \right\} / (k/2) \quad (3.41)$$

For convenience, define the following variables

$$\begin{aligned} Z_{1k} &= 2(a_k^r \sigma_k - a_k^i \omega_k) \\ Z_{2k} &= 2(i\omega_0) a_k^r \\ Z_{3k} &= (\sigma_k)^2 + (\omega_k)^2 - (i\omega_0)^2 \\ Z_{4k} &= -2(i\omega_0) \sigma_k \end{aligned} \quad (3.42)$$

Separating equation (3.41) into real and imaginary parts and substituting relations (3.42) results in:

$$R'^r = \left\{ \sum_{i=1}^{k/2} \left[h_i^r - \sum_{k=1}^n \frac{Z_{1k} Z_{3k}}{(Z_{3k})^2 + (Z_{4k})^2} - \frac{Z_{2k} Z_{4k}}{(Z_{3k})^2 + (Z_{4k})^2} \right] \right\} / (k/2)$$

$$R'_i = \left\{ \sum_{i=1}^{k/2} \left[h_i^i - \sum_{k=1}^n \frac{Z_{2k}Z_{3k}}{(Z_{3k})^2 + (Z_{4k})^2} - \frac{Z_{1k}Z_{4k}}{(Z_{3k})^2 + (Z_{4k})^2} \right] \right\} / (k/2) \quad (3.43)$$

Now then, write equation (3.24) to include the constant R' .

$$R_m = \frac{a_m^*}{j\omega - s_m^*} + \sum_{\substack{k=1 \\ k \neq m}}^n \left[\frac{a_k}{j\omega - s_k} + \frac{a_k^*}{j\omega - s_k^*} \right] + R' \quad (3.44)$$

Again, this equation can be separated into real and imaginary parts for convenience of computations. Define the following:

$$\begin{aligned} Z_{5k} &= 2\omega a_k^r \\ Z_{6k} &= (\sigma_k)^2 + (\omega_k)^2 - \omega^2 \\ Z_{7k} &= -2\omega\sigma_k \end{aligned} \quad (3.45)$$

Then equation (3.44) can be written as:

$$\begin{aligned}
 R_m^r &= \frac{\sigma_m a_m^r + a_m^i(\omega + \omega_m)}{(\sigma_m)^2 + (\omega + \omega_m)^2} \\
 &+ \sum_{\substack{k=1 \\ k \neq m}}^n \left[\frac{Z_{1k}Z_{6k} - Z_{5k}Z_{7k}}{(Z_{6k})^2 + (Z_{7k})^2} \right] + R^r \\
 R_m^i &= \frac{\sigma_m a_m^i - a_m^r(\omega + \omega_m)}{(\sigma_m)^2 + (\omega + \omega_m)^2} \\
 &+ \sum_{\substack{k=1 \\ k \neq m}}^n \left[\frac{Z_{5k}Z_{6k} + Z_{1k}Z_{7k}}{(Z_{6k})^2 + (Z_{7k})^2} \right] + R^i
 \end{aligned} \tag{3.46}$$

The curve fitting now uses equation (3.46) in lieu of equation (3.24). Again, R_m is assumed initially to be zero and then values for s_m and a_m can be computed. Then an iterative solution can be arrived at using equations (3.34) through (3.37), (3.43), and (3.46). A computer algorithm using these equations can be found in Appendix B.

This technique works fine for systems with

light to moderate damping. When there is heavy modal overlap due to closely spaced resonant frequencies, but with light damping, the technique again works reasonably well. However if there are closely spaced frequencies and the damping ratios approach 0.2, then the error in the estimated parameters begins to get too large. A discussion on the error versus damping ratio is presented in Chapter IV in conjunction with the example problems.

3.3.2 Curve Fitting of Quadrature Response

As previously mentioned, the total response curve fitting technique works well when the degree of modal overlap is light. As the degree of overlap increases, this method yields greater errors. One method which provides more accurate results is to curve fit the quadrature, or imaginary, part of the transfer function. The main reason for choosing the quadrature response is the rapid change it displays near resonant frequencies. The quadrature response peaks much sharper at a resonance as compared to the total response curve.

In this section, the imaginary curve fit algorithm will be developed. The assumptions used appear

not to have any degrading effects.

Consider the summation of equation (3.22).

After expanding into real and imaginary parts the imaginary part can be written as:

$$\text{Im } H(j\omega) = \sum_{k=1}^n - \frac{2\omega\alpha_k\sigma_k^2 - 2\omega\alpha_k\omega_k^2 + 2\alpha_k\omega^3 - 4\omega\beta_k\sigma_k\omega_k}{\sigma_k^4 + \omega_k^4 + \omega^4 + 2\sigma_k^2\omega_k^2 + 2\sigma_k^2\omega^2 - 2\omega_k^2\omega^2} \quad (3.47)$$

where

$$a_k = \alpha_k + j\beta_k$$

$$s_k = -\sigma_k + j\omega_k$$

Due to the form of the above equation, a closed form solution for the unknown parameters is not feasible.

A Newton - Raphson technique can be applied in the following manner. Define the following function

$$g = \sum_{k=1}^n - \frac{2\omega\alpha_k\sigma_k^2 - 2\omega\alpha_k\omega_k^2 + 2\alpha_k\omega^3 - 4\omega\beta_k\sigma_k\omega_k}{\sigma_k^4 + \omega_k^4 + \omega^4 + 2\sigma_k^2\omega_k^2 + 2\sigma_k^2\omega^2 - 2\omega_k^2\omega^2} - \text{Im}[H(j\omega)] \quad (3.48)$$

This function would be equal to zero if the exact values of α_k , β_k , σ_k , and ω_k were known. If initial

estimates were available for these parameters then an iterative technique could be applied to improve the estimates. It can be seen from equation (3.47) that if the parameters σ_k and ω_k are known then equation (3.47) becomes a linear function of α_k and β_k , i.e., the residues (a_k). Thus, it would only be necessary to provide initial estimates for natural frequencies and damping ratios. The estimates for the residues (a_k) are then obtained by using a Gaussian elimination technique on equation (3.47) evaluated at $2n$ frequency points (preferably two points on each peak).

In order to define an iterative technique for the solution of equation (3.47), the function g (equation (3.48)) can be rewritten as

$$g = f(\sigma_m, \omega_m, \alpha_m, \beta_m) + f'(\sigma_k, \omega_k, \alpha_k, \beta_k) - h^i \quad (3.49)$$

where

$f(\sigma_m, \omega_m, \alpha_m, \beta_m)$ = the term of equation (3.48) associated with the m^{th} pole

$f'(\sigma_k, \omega_k, \alpha_k, \beta_k)$ = the summation of all terms in equation (3.48) except for the term associated with the m^{th} pole

$$h^i = \text{Im}[h(j\omega)]$$

Using initial estimates for the unknown parameters, the function defined by equation (3.49) can be expanded in a Taylor series expansion. Neglecting the second and higher order terms, and assuming that the function f' is a constant at frequencies near the m^{th} resonant frequency, the expansion becomes:

$$\begin{aligned} g_{n+1} = g_n &+ \left. \frac{\partial g}{\partial \sigma_m} \right|_n (\sigma_{m_{n+1}} - \sigma_{m_n}) + \left. \frac{\partial g}{\partial \omega_m} \right|_n (\omega_{m_{n+1}} - \omega_{m_n}) \\ &+ \left. \frac{\partial g}{\partial \alpha_m} \right|_n (\alpha_{m_{n+1}} - \alpha_{m_n}) + \left. \frac{\partial g}{\partial \beta_m} \right|_n (\beta_{m_{n+1}} - \beta_{m_n}) \end{aligned} \quad (3.50)$$

where the n denotes the initial estimate and $n + 1$ is the improved estimate. The partial derivatives are evaluated at the initial estimates. Since g_{n+1} should equal zero, equation (3.50) can be written as:

$$\begin{aligned} -g_n = &\left. \frac{\partial g}{\partial \sigma_m} \right|_n (\sigma_{m_{n+1}} - \sigma_{m_n}) + \left. \frac{\partial g}{\partial \omega_m} \right|_n (\omega_{m_{n+1}} - \omega_{m_n}) \\ &+ \left. \frac{\partial g}{\partial \alpha_m} \right|_n (\alpha_{m_{n+1}} - \alpha_{m_n}) + \left. \frac{\partial g}{\partial \beta_m} \right|_n (\beta_{m_{n+1}} - \beta_{m_n}) \end{aligned} \quad (3.51)$$

If equation (3.51) is written at four frequency points on the m^{th} peak then a matrix equation can be set up as follows:

$$\begin{Bmatrix} g_1 \\ g_2 \\ g_3 \\ g_4 \end{Bmatrix}_n = \begin{bmatrix} \frac{\partial g_1}{\partial \sigma_m} & \frac{\partial g_1}{\partial \omega_m} & \frac{\partial g_1}{\partial a_m} & \frac{\partial g_1}{\partial b_m} \\ \frac{\partial g_2}{\partial \sigma_m} & \frac{\partial g_2}{\partial \omega_m} & \frac{\partial g_2}{\partial a_m} & \frac{\partial g_2}{\partial b_m} \\ \frac{\partial g_3}{\partial \sigma_m} & \frac{\partial g_3}{\partial \omega_m} & \frac{\partial g_3}{\partial a_m} & \frac{\partial g_3}{\partial b_m} \\ \frac{\partial g_4}{\partial \sigma_m} & \frac{\partial g_4}{\partial \omega_m} & \frac{\partial g_4}{\partial a_m} & \frac{\partial g_4}{\partial b_m} \end{bmatrix}_n \begin{Bmatrix} \sigma_m \\ \omega_m \\ a_m \\ b_m \end{Bmatrix}_n - \begin{Bmatrix} \sigma_m \\ \omega_m \\ a_m \\ b_m \end{Bmatrix}_{n+1} \quad (3.52)$$

Define the following matrices:

$$\underline{x} = \begin{Bmatrix} \sigma_m \\ \omega_m \\ a_m \\ b_m \end{Bmatrix}$$

$$\underline{g} = \begin{Bmatrix} g_1 \\ g_2 \\ g_3 \\ g_4 \end{Bmatrix}$$

$$\underline{J} = \begin{bmatrix} \frac{\partial g_1}{\partial \sigma_m} & \frac{\partial g_1}{\partial \omega_m} & \frac{\partial g_1}{\partial a_m} & \frac{\partial g_1}{\partial b_m} \\ \frac{\partial g_2}{\partial \sigma_m} & \frac{\partial g_2}{\partial \omega_m} & \frac{\partial g_2}{\partial a_m} & \frac{\partial g_2}{\partial b_m} \\ \frac{\partial g_3}{\partial \sigma_m} & \frac{\partial g_3}{\partial \omega_m} & \frac{\partial g_3}{\partial a_m} & \frac{\partial g_3}{\partial b_m} \\ \frac{\partial g_4}{\partial \sigma_m} & \frac{\partial g_4}{\partial \omega_m} & \frac{\partial g_4}{\partial a_m} & \frac{\partial g_4}{\partial b_m} \end{bmatrix}$$

Using these definitions, equation (3.52) can be written as:

$$\underline{x}_{n+1} = \underline{x}_n - \underline{J}^{-1} \underline{g}_n \quad (3.53)$$

Thus, with initial estimates for the damping ratios and natural frequencies, equation (3.47) can be solved for initial estimates of the residues. Once initial estimates are obtained for natural frequencies, damping ratios, and residues, then equation (3.53) can be used to improve the estimates. In order to get the initial estimates for the natural frequencies and damping ratios which define the system poles, use was made of the method of Kennedy and Pancu discussed earlier. As will be shown later, this method provides fair estimates for the system poles, but not necessarily the mode shapes. For all cases considered in this

thesis, the circle fit method provided estimates with sufficient accuracy for this algorithm to converge.

The imaginary curve fitting technique provides very accurate estimates for the modal parameters for systems with a light degree of modal overlap. As the degree of modal overlap increases, more accurate initial estimates are required for this method to converge. As the damping ratio approaches 0.2 with resonant frequencies closely spaced, this method becomes unstable if the initial estimates for natural frequency and damping ratio are in error by more than 10%.

3.4 Summary

Each of these methods has its advantages and limitations. Chapter IV will present two example problems, each one analyzed by each curve fit method discussed in Sections 3.2.2, 3.3.1, and 3.3.2. The results are summarized to show the advantages and limitations of each method.

CHAPTER IV
EXAMPLES OF CURVE FITTING TECHNIQUES

4.1 Introduction

This chapter will be devoted to exploring the use of the curve fitting techniques described in Chapter III on an example problem. The problem to be considered will be the two degree of freedom system shown in Figure 4.1.

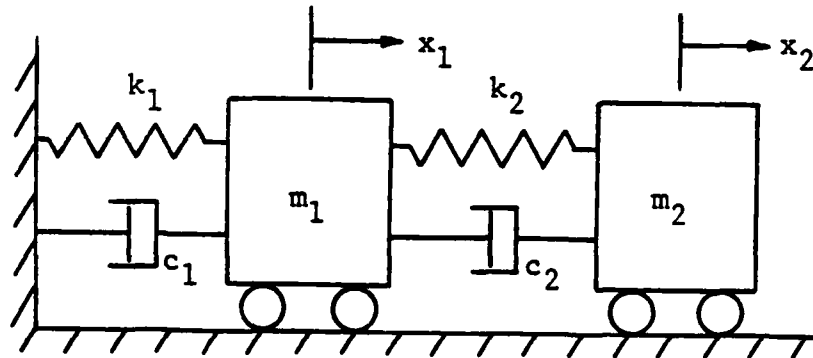


Figure 4.1. Example Problem

This system will be used for two example problems, one with the system poles separated widely and one with the poles close together. The estimates obtained in each case will be compared to the actual results in

order to show the usefulness and extent of each curve fit method.

4.2 Example Problem One

Define the variables of Figure 4.1 as:

$$\begin{array}{ll} m_1 = 1 & m_2 = 6 \\ k_1 = 100 & k_2 = 6 \\ c_1 = .1 & c_2 = .1 \end{array}$$

For this system, the actual values for the modal parameters as computed via a complex eigen-solver routine are:

$$\begin{array}{ll} \omega_1 = 0.97103 \text{ rad/sec} & \omega_2 = 10.29834 \text{ rad/sec} \\ \zeta_1 = 0.00765 & \zeta_2 = 0.00980 \end{array}$$

$$\text{mode 1} = \left\{ \begin{array}{ll} 0.05711 & / -359.17^\circ \\ 1.0 & / 0^\circ \end{array} \right\}$$

$$\text{mode 2} = \left\{ \begin{array}{ll} 1.0 & / 0^\circ \\ 0.00964 & / -171.27^\circ \end{array} \right\}$$

Recall that the transfer matrix can be written as:

$$H(s) = \begin{bmatrix} h_{11}(s) & h_{12}(s) \\ h_{21}(s) & h_{22}(s) \end{bmatrix}$$

If the frequency response functions $h_{11}(j\omega)$ and $h_{21}(j\omega)$ are measured, then all of the modal parameter estimations may be obtained. In all of the cases to follow, h_{11} and h_{21} are used to determine the estimates of the natural frequencies, damping ratios, and mode shapes.

4.2.1 Method of Kennedy and Pancu (Circle Fit)

The algorithm in Appendix A was used to compute the estimations shown in Table 4.1. Immediately the

Table 4.1

PARAMETER	ESTIMATION	ACTUAL VALUE	% ERROR
ω_1	0.96000	0.97103	1.14
ζ_1	0.03577	0.00765	367.58
ω_2	10.29800	10.29834	0.003
ζ_2	0.00980	0.00980	0.0
mode 1	$\begin{bmatrix} 0.05711 & /-359.16^\circ \\ 1 & / 0^\circ \end{bmatrix}$	$\begin{bmatrix} 0.05711 & /-359.17^\circ \\ 1 & / 0^\circ \end{bmatrix}$	$0.0M^*$ $0.03P^*$
mode 2	$\begin{bmatrix} 1 & / 0^\circ \\ 0.00965 & /-171.26^\circ \end{bmatrix}$	$\begin{bmatrix} 1 & / 0^\circ \\ 0.00964 & /-171.27^\circ \end{bmatrix}$	$0.11M$ $0.01P$

*M = Magnitude P = Phase

error for ζ_1 stands out. This gross error can be readily explained, and is a good example of one of the problems associated with this method. This error was the result of insufficient frequency resolution in the frequency response data. The above problem was reworked with better resolution by looking only at the frequencies near ω_1 . This provided a 0.01% error in ζ_1 .

One other problem associated with this method is that of one mode dominating the other nearby modes. For this problem, even though mode 2 dominates, it is separated far enough in frequency so as not to interact with mode 1. Figure 4.2 is the polar plot for the h_{11} frequency response of this problem. It appears at first to be a plot of a single degree of freedom system, however, a closer look reveals a very small response circle near the origin. This domination can be seen more easily on the log-magnitude plot of Figure 4.3. This type of domination can be a problem if the natural frequencies are close together.

The damping ratio in this problem was varied from approximately 0.008 to approximately 0.20. The exact solutions are tabulated in Appendix D.1 and the curve fit estimations are given in Appendix D.2. As

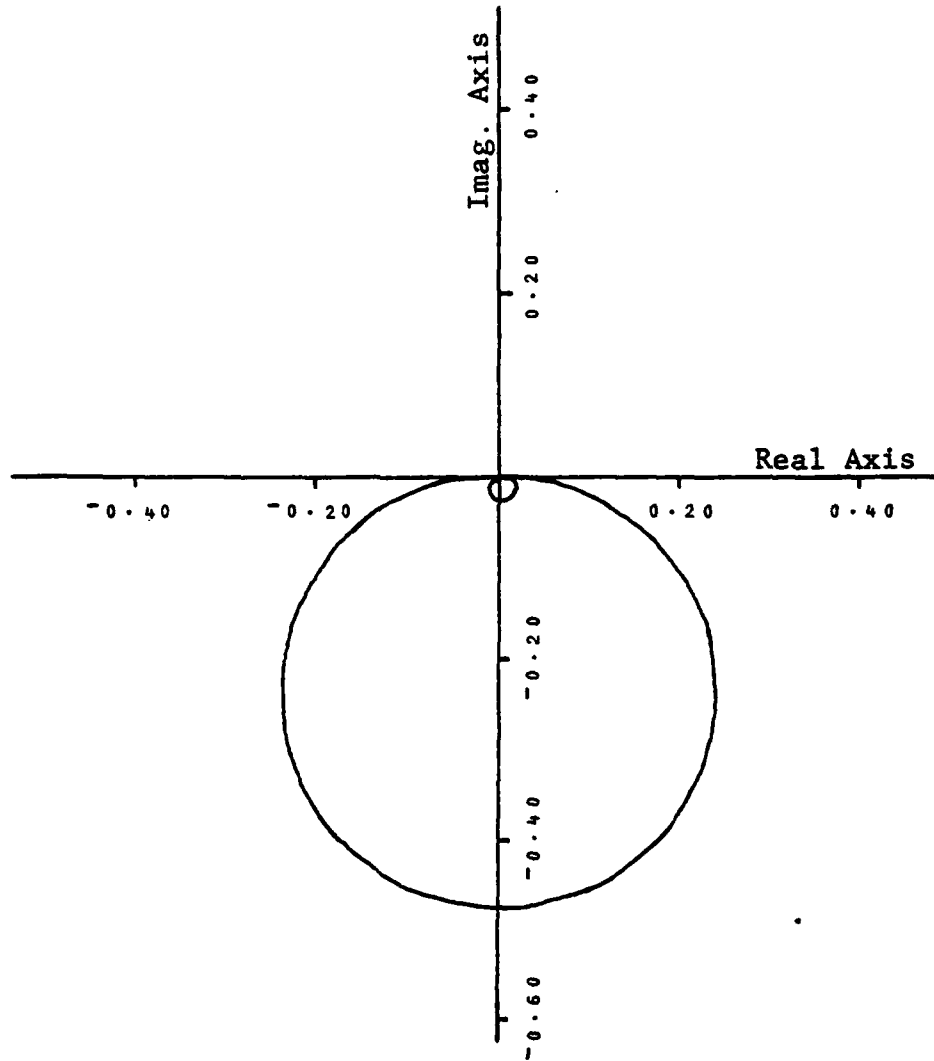


Figure 4.2. Polar Plot of h_{11}

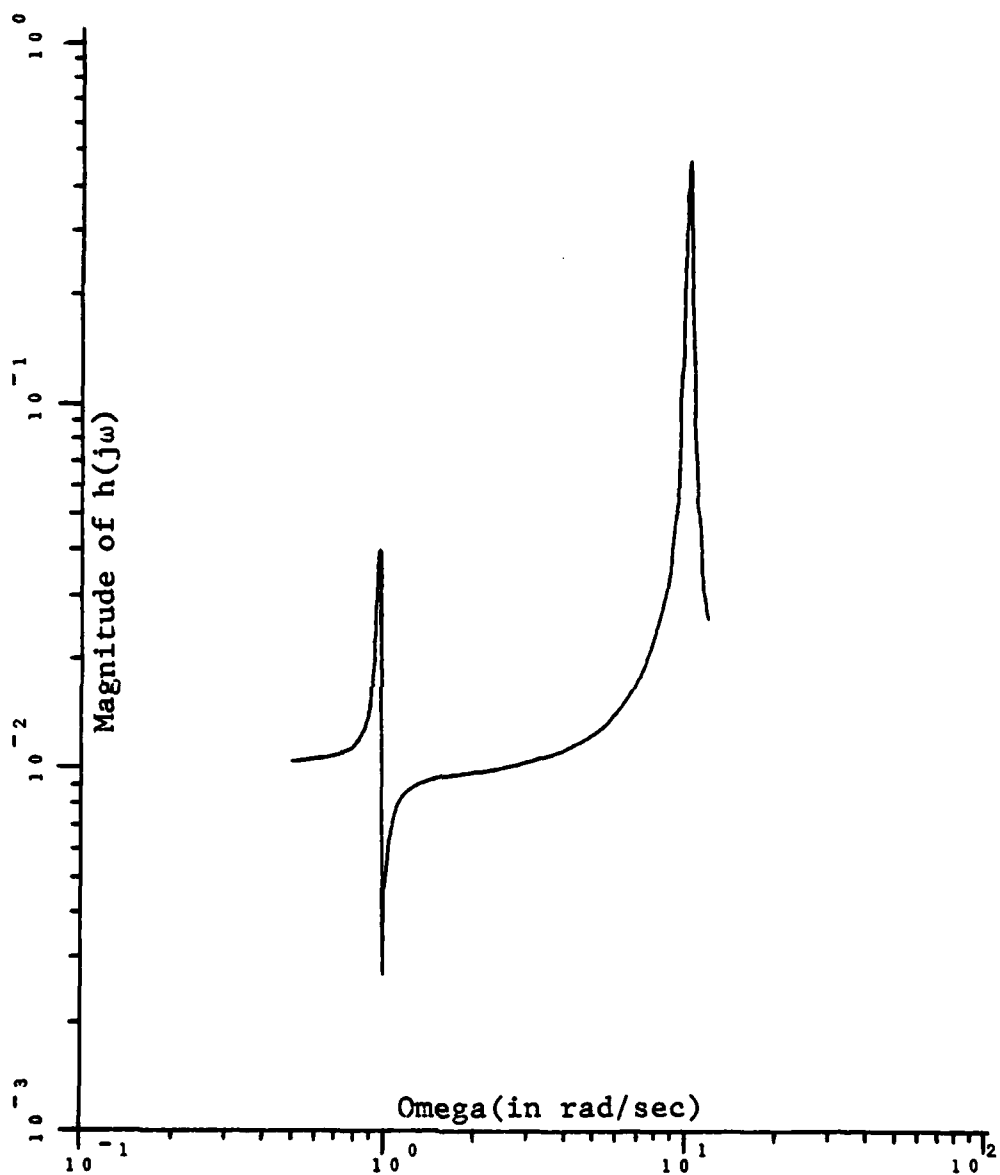


Figure 4.3. Log-Magnitude Plot of h_{11}

a summary of the results, the maximum errors in frequency, damping, and mode shape estimations are plotted in Figure 4.4 as a function of damping ratio. In

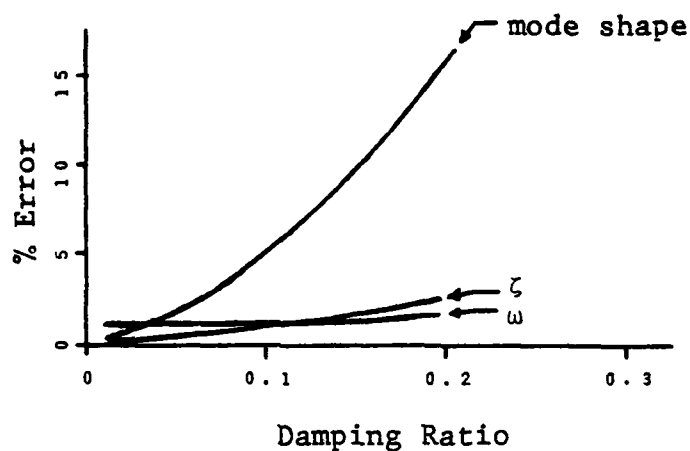


Figure 4.4. Percent Error vs Damping Ratio Using Circle Fit, Poles Separated ($\omega_1 = 10.298$ rad/sec, $\omega_2 = 0.971$ rad/sec)

general, as the damping increases, so do the errors in the estimations. The very large error for ζ_1 , discussed earlier (see Table 4.1), was not plotted because of the misleading effect it would have in the error plot.

It should be noted that the error is dependent, not only on the damping, but also on the frequency resolution, as was seen earlier. As the frequency reso-

lution is increased, the errors decrease. However, in this study the frequency resolution was kept constant and the error evaluated only as a function of damping. The frequency resolution used for this problem was approximately 0.02 rad/sec.

4.2.2 Complex Curve Fit

The algorithm in Appendix B was used for these computations. The results outlined in Table 4.2 were

Table 4.2

PARAMETER	ESTIMATION	ACTUAL VALUE	% ERROR
ω_1	0.97103	0.97103	0.0
ζ_1	0.00765	0.00765	0.0
ω_2	10.29834	10.29834	0.0
ζ_2	0.00980	0.00980	0.0
mode	$\left[\begin{array}{l} 0.05712 \ / \ -359.17^\circ \\ 1 \ / \ 0^\circ \end{array} \right]$	$\left[\begin{array}{l} 0.05711 \ / \ -359.17^\circ \\ 1 \ / \ 0^\circ \end{array} \right]$	0.02M
1			0.0P
mode	$\left[\begin{array}{l} 1 \ / \ 0^\circ \\ 0.01243 \ / \ -176.35^\circ \end{array} \right]$	$\left[\begin{array}{l} 1 \ / \ 0^\circ \\ 0.00964 \ / \ -171.27^\circ \end{array} \right]$	28.94M
2			2.97P

obtained using the original values of damping as defined in Section 4.2. From Table 4.2 it can be seen that this method provides good estimates for natural frequencies and damping ratios. However, the error

in the 2nd mode shape gets larger as damping increases. It is noted that the algorithm converged very slowly on frequency response h_{21} . This points out one of the problems with this technique. As noted earlier, one mode dominates in this problem. When this situation occurs, the initial estimates provided by the two point estimation are not very accurate. As a result, the convergence is either slow or non-existent. This same problem can be encountered when the damping ratio is increased.

As in the previous section, the damping ratio was varied from approximately 0.008 to 0.20 and the results tabulated in Appendix D.3. Figure 4.5 is a plot of the error vs damping for this algorithm. The error in the mode shapes associated with the lack of convergence were not plotted in order to avoid misrepresentation of the error vs damping. Again, as the damping increased, the errors, in general, increased for a fixed frequency resolution.

It appears that the main problem with this method is that the initial estimates for the residues are sometimes not good enough to provide convergence. The initial estimates for the residues are calculated using the original assumption that off-

resonant modes do not contribute to the transfer function at any given resonance. This assumption is questionable under conditions of heavy modal overlap or

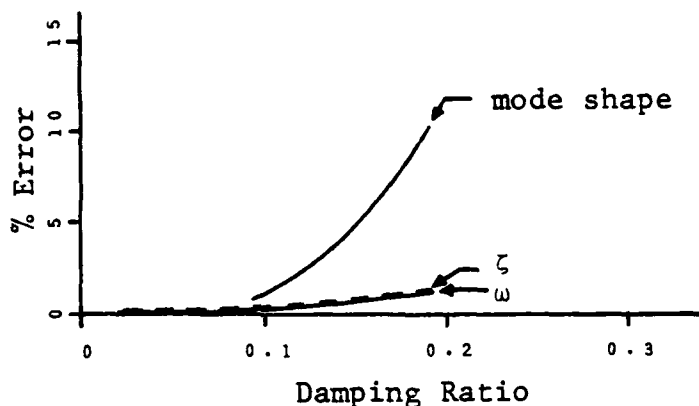


Figure 4.5. Percent Error vs Damping Ratio Using Complex Curve Fit, Poles Separated ($\omega_1 = 10.298$ rad/sec, $\omega_2 = 0.971$ rad/sec)

where one mode is dominant. The initial residue estimates could possibly be improved by the use of a technique similar to that used in the next section.

4.2.3 Curve Fit of Imaginary Part of $H(j\omega)$

The algorithm of Appendix C was used to compute the estimates in this section. The convergence of this technique is highly dependent upon high grade initial parameter estimates. For this algorithm, es-

timates are required for the natural frequencies and damping ratios only, since the algorithm computes the initial estimates for the residues. If the initial estimates of damping and natural frequency are more than 10% in error, the algorithm may diverge using this technique. For the purpose of this thesis, the initial estimates were taken from the method of Kennedy and Pancu (Circle Fit, Section 4.2.1). Except for the case of inadequate frequency resolution, the circle fit method gave good results for natural frequencies and damping ratios. The results obtained using the imaginary curve fit to improve the initial estimates are shown in Table 4.3.

Table 4.3

PARAMETER	ESTIMATION	ACTUAL VALUE	% ERROR
ω_1	0.97103	0.97103	0.0
ζ_1	0.00765	0.00765	0.0
ω_2	10.29834	10.29834	0.0
ζ_2	0.00980	0.00980	0.0
mode	$\left[\begin{array}{c} 0.05712 \ / \ -359.17^\circ \\ 1 \ / \ 0^\circ \end{array} \right]$	$\left[\begin{array}{c} 0.05711 \ / \ -359.17^\circ \\ 1 \ / \ 0^\circ \end{array} \right]$	0.01M
1			0.0P
mode	$\left[\begin{array}{c} 1 \ / \ 0^\circ \\ 0.00964 \ / \ -171.29^\circ \end{array} \right]$	$\left[\begin{array}{c} 1 \ / \ 0^\circ \\ 0.00964 \ / \ -171.27^\circ \end{array} \right]$	0.0M
2			0.01P

As in the previous sections, the damping ratio was varied in the approximate range of 0.008 to 0.20 and the results tabulated in Appendix D.4. Figure 4.6 plots the error in the parameter estimation vs damping

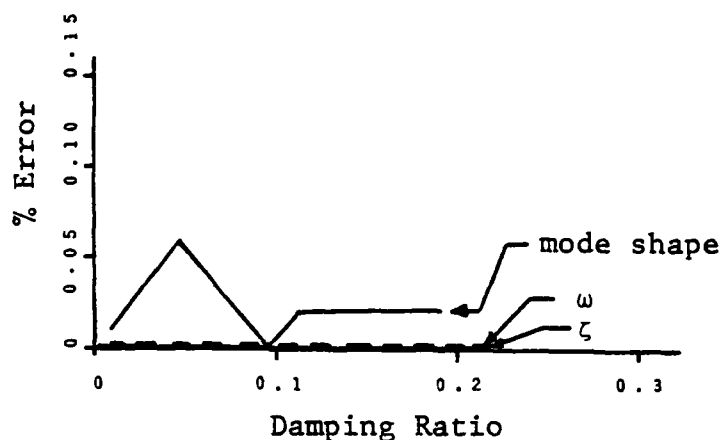


Figure 4.6. Percent Error vs Damping Ratio Using Imaginary Curve Fit, Poles Separated ($\omega_1 = 10.298$ rad/sec, $\omega_2 = 0.971$ rad/sec)

ratio. The broken line shown for the mode shape plot was drawn that way because of the magnitudes of the error. Notice the drastic change in the scale for % error. If this mode shape error would have been plotted on one of the previous plots (Figures 4.4 or 4.5) it would have appeared as a straight line very near 0% error. In fact, if the error criterion were based on an accuracy of only three decimal places instead of

five (as used in this study) then there would be 0% error for all parameter estimations in this problem.

The damping ratio was not increased any further because of the difficulty in obtaining natural frequencies and damping ratios. This is an area that needs further research before the full limits of the imaginary curve fit algorithm can be tested.

It can be seen that this method is more desirable than the previous two methods, especially if the mode shapes are of interest.

4.3 Example Problem Two

Using the same system as described in Figure 4.1, define the following variables:

$$\begin{array}{ll} m_1 = 3 & m_2 = 1 \\ k_1 = 36 & k_2 = 6 \\ c_1 = .15 & c_2 = 0.05 \end{array}$$

For this system, the actual values for the modal parameters as computed via a complex eigen solver routine are:

$$\omega_1 = 2.16993 \text{ rad/sec} \quad \omega_2 = 3.91039 \text{ rad/sec}$$

$$\zeta_1 = 0.00764$$

$$\zeta_2 = 0.01068$$

$$\text{mode 1} = \left\{ \begin{array}{l} 0.21526 \quad /-359.41^\circ \\ 1 \quad \quad \quad / \quad 0^\circ \end{array} \right\}$$

$$\text{mode 2} = \left\{ \begin{array}{l} 1 \quad \quad \quad / \quad 0^\circ \\ 0.64593 \quad /-178.94^\circ \end{array} \right\}$$

The main difference between this problem and problem one is spacing of the system poles. For this problem the poles are close together compared to the separation in problem one.

As in the previous example problem, the frequency response functions h_{11} and h_{21} were used to estimate the modal parameters. The frequency resolution in this problem was approximately 0.01 rad/sec.

4.3.1 Method of Kennedy and Pancu (Circle Fit)

As in Section 4.2.1, the estimates for the modal parameters were computed and the results presented in Table 4.4. One can immediately see that the estimates are very good. The frequency resolution was sufficient in this case to provide good estimates, with the damping at a low level. However, as the amount of damping increased, the accuracy dropped off

rapidly. The damping ratio was varied over the approximate range of 0.008 to 0.20 and the results

Table 4.4

PARAMETER	ESTIMATION	ACTUAL VALUE	% ERROR
ω_1	2.17000	2.16993	0.003
ζ_1	0.00763	0.00764	0.13
ω_2	3.91000	3.91039	0.01
ζ_2	0.01068	0.01068	0.0
mode 1	$\begin{bmatrix} 0.21510 & /-359.41^\circ \\ 1 & / 0^\circ \end{bmatrix}$	$\begin{bmatrix} 0.21526 & /-359.41^\circ \\ 1 & / 0^\circ \end{bmatrix}$	0.07M 0.0P
mode 2	$\begin{bmatrix} 1 & / 0^\circ \\ 0.64733 & /-178.94^\circ \end{bmatrix}$	$\begin{bmatrix} 1 & / 0^\circ \\ 0.64593 & /-178.94^\circ \end{bmatrix}$	0.22M 0.0P

tabulated in Appendix D.6. For purposes of comparison, the exact solutions are tabulated in Appendix D.5. Figure 4.7 shows how the errors increased with damping. The errors in this problem are larger than those in the first example because the poles are closer together and the modes interact more with each other. Figure 4.8 shows the polar plot of h_{11} with a damping ratio of approximately 0.008. Figure 4.9 is the same frequency response function except that the damping ratio is now approximately 0.20. Figures 4.10 and 4.11 are the log-magnitude plots of the functions rep-

resented in Figures 4.8 and 4.9, respectively. The

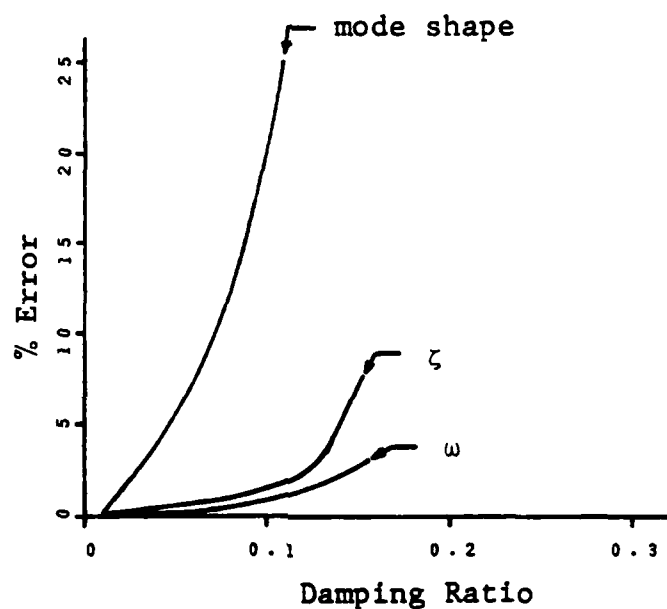


Figure 4.7. Percent Error vs Damping Using Circle Fit, Poles Close
 $(\omega_1 = 2.170 \text{ rad/sec,}$
 $\omega_2 = 3.910 \text{ rad/sec})$

interaction of the two modes can be clearly seen in these figures. This interaction poses a problem when using this technique, because the responses tend to not approximate a circle at points removed from the natural frequency. This causes a circle of improper dimensions to be fit through the data, thus giving rise to larger errors in damping ratios and mode shapes.

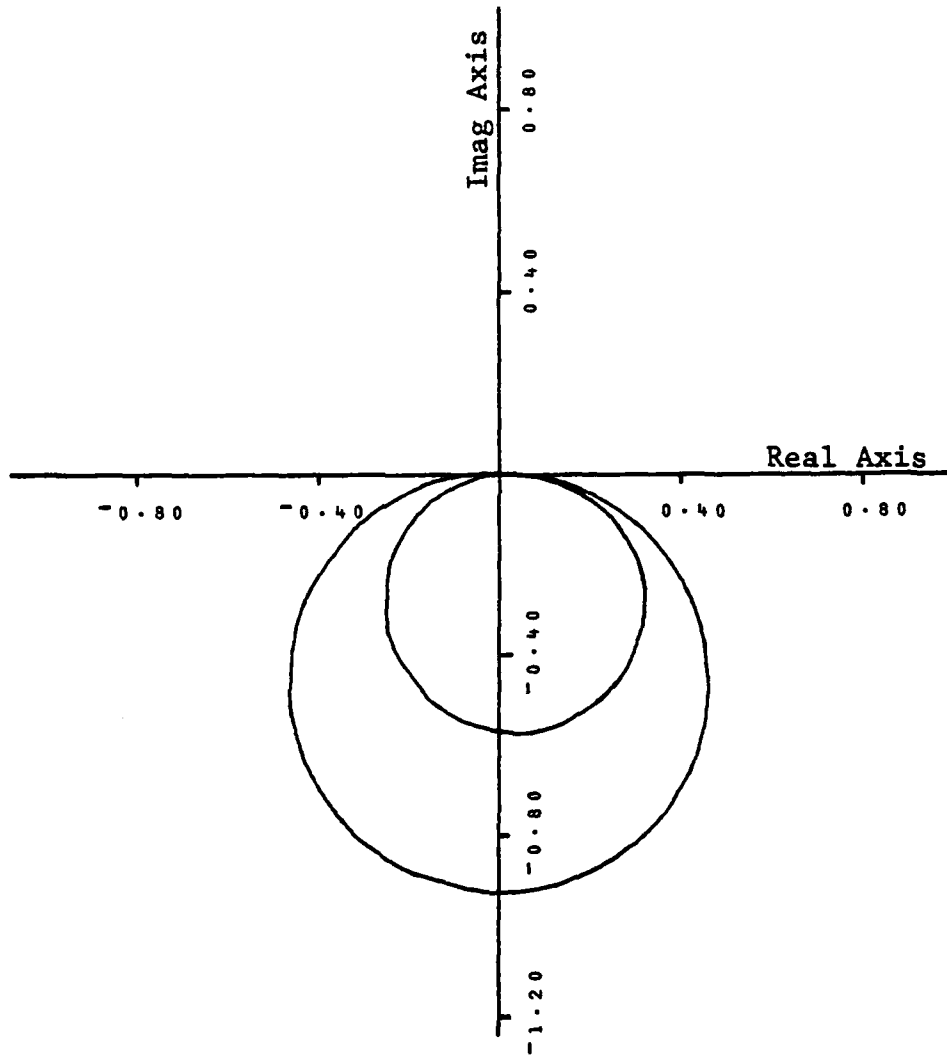


Figure 4.8. Polar Plot of $h_{11}(zeta = 0.008)$

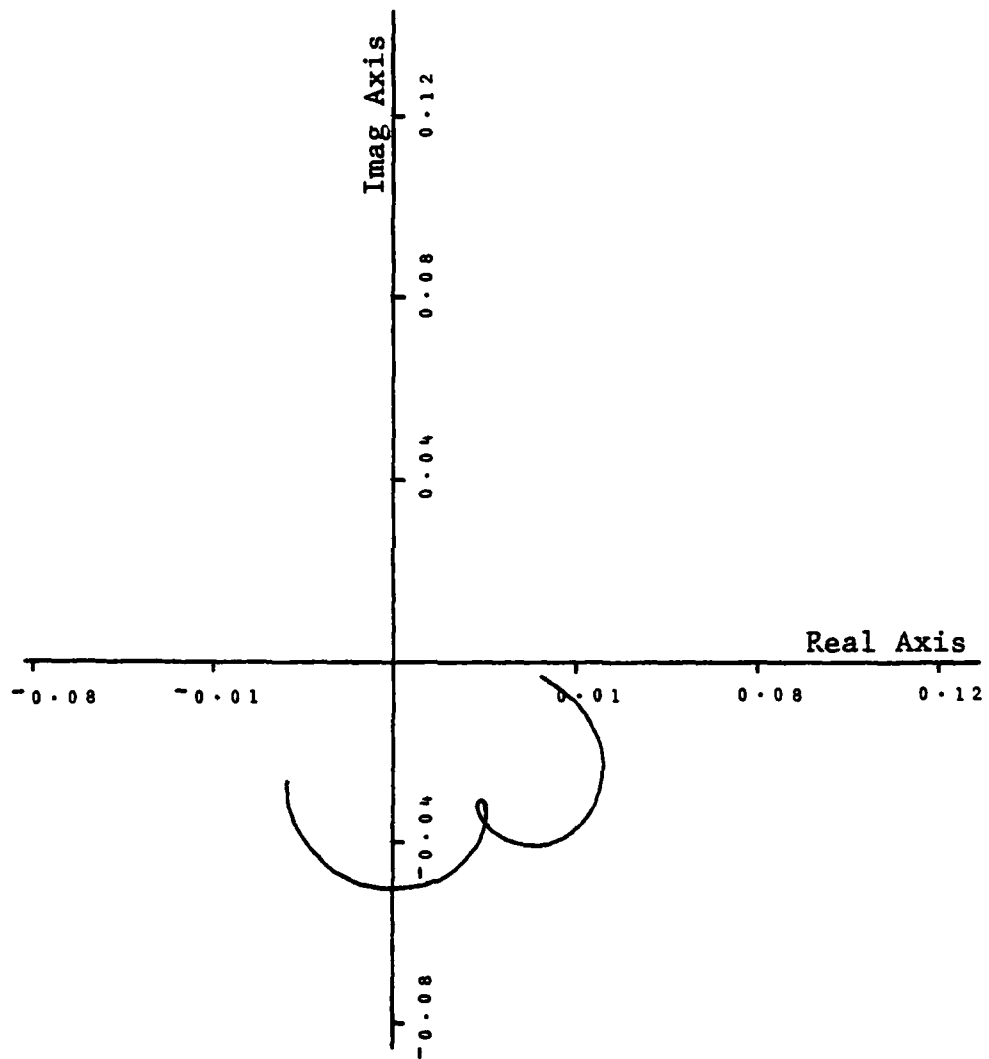


Figure 4.9. Polar Plot of $h_{11}(\zeta = 0.20)$

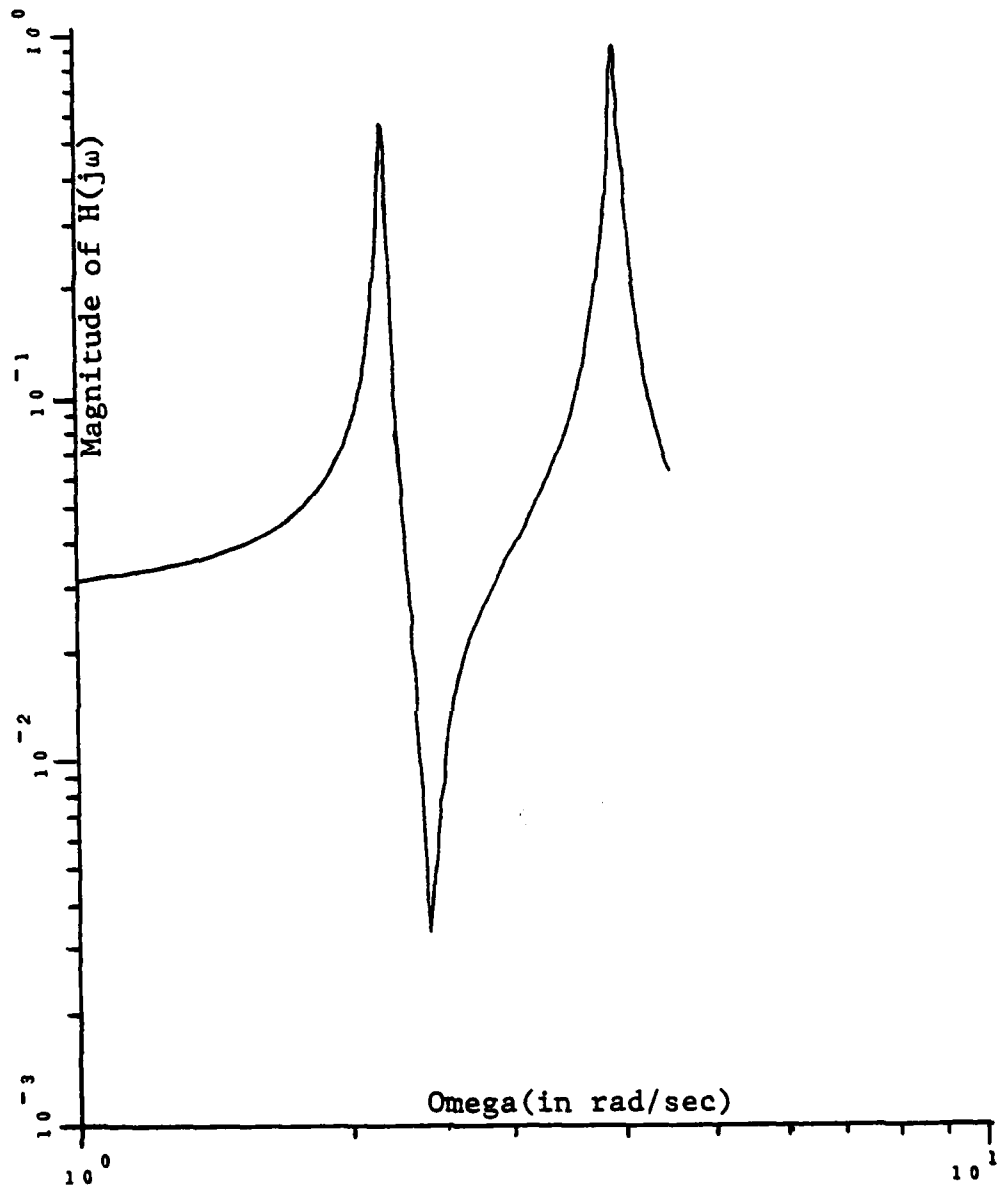


Figure 4.10. Log-Magnitude Plot
of $h_{11}(\zeta = 0.008)$

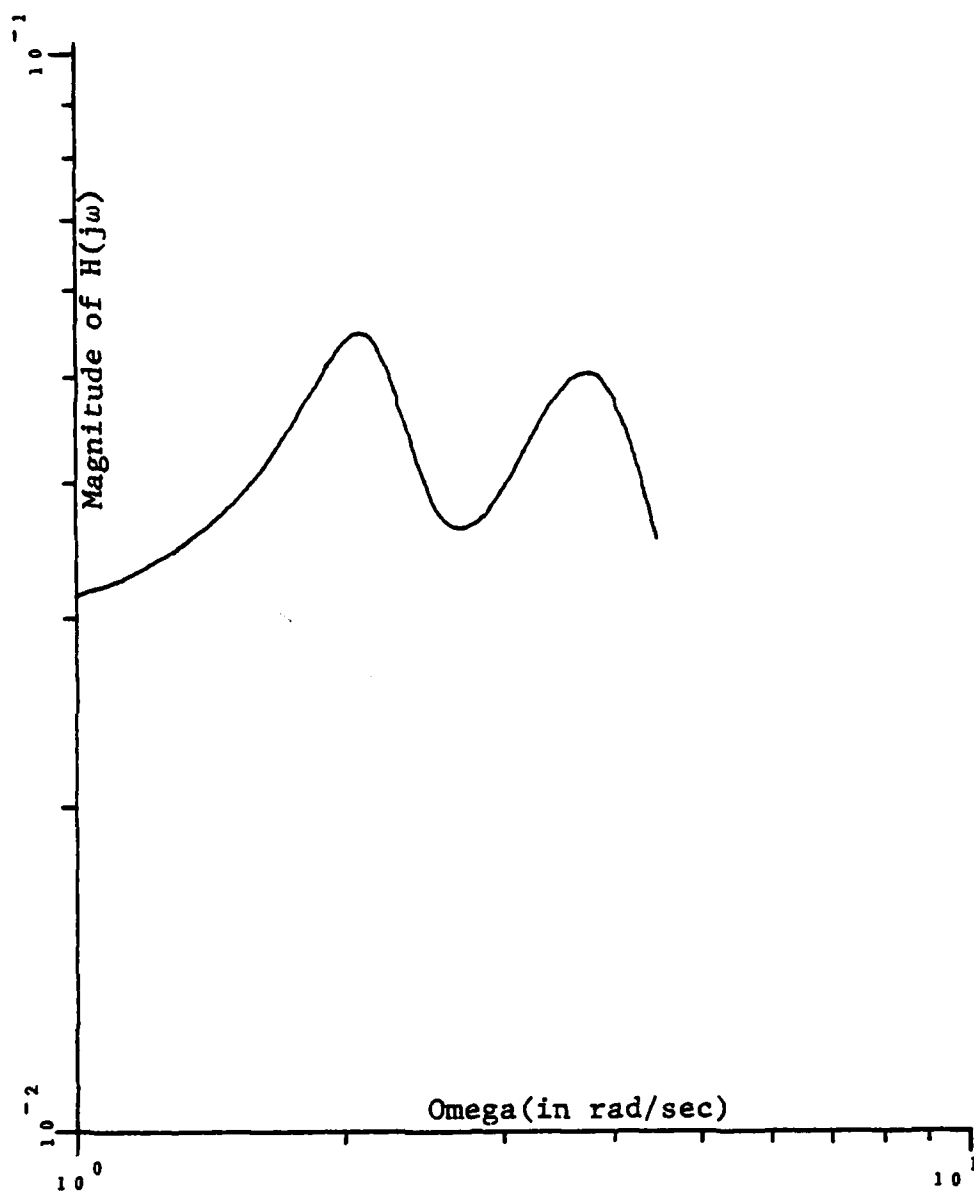


Figure 4.11. Log-Magnitude Plot of $h_{11}(\zeta = 0.20)$

4.3.2 Complex Curve Fit

The estimates using this technique are given in Table 4.5 for the original damping defined in Section 4.3. As the damping was increased from approximately

Table 4.5

PARAMETER	ESTIMATION	ACTUAL VALUE	% ERROR
ω_1	2.16993	2.16993	0.0
ζ_1	0.00764	0.00764	0.0
ω_2	3.91038	3.91039	0.002
ζ_2	0.01068	0.01068	0.0
mode 1	$\begin{bmatrix} 0.21533 & /-359.41^\circ \\ 1 & / 0^\circ \end{bmatrix}$	$\begin{bmatrix} 0.21526 & /-359.41^\circ \\ 1 & / 0^\circ \end{bmatrix}$	0.03M 0.0P
mode 2	$\begin{bmatrix} 1 & / 0^\circ \\ 0.64532 & /-178.95^\circ \end{bmatrix}$	$\begin{bmatrix} 1 & / 0^\circ \\ 0.64593 & /-178.94^\circ \end{bmatrix}$	0.09M 0.01P

0.008 to approximately 0.20 the errors also increased (see Appendix D.7). The plot of error vs damping in Figure 4.12 shows rapid increase in error as the damping increased. As discussed in Section 4.2.2, the assumptions used in this method are questionable with heavy modal overlap. Figures 4.10 and 4.11 show that there is considerable overlap between the two modes, which explains the large increase in error with increase in the damping ratio.

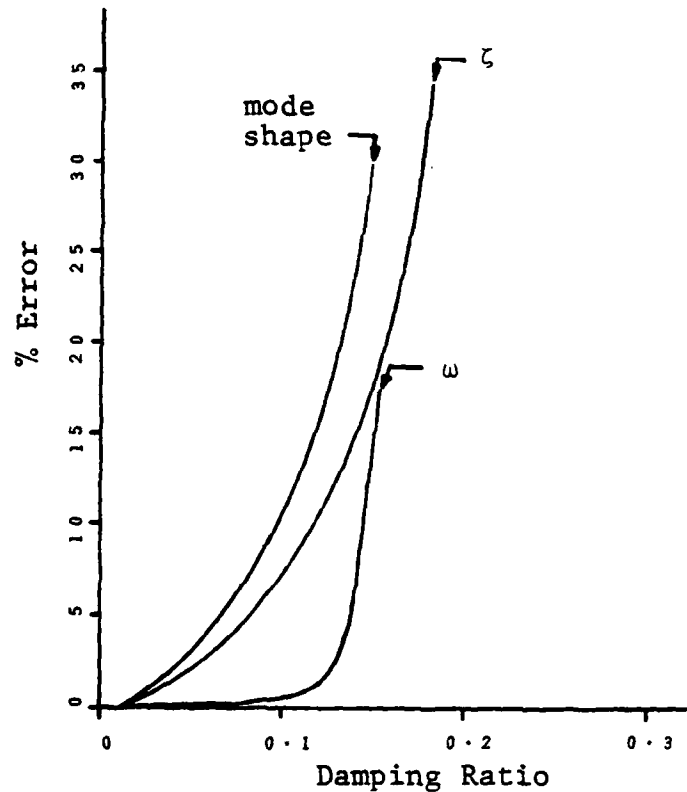


Figure 4.12. Percent Error vs Damping Ratio Using Complex Curve Fit, Poles Close ($\omega_1 = 2.17$ rad/sec, $\omega_2 = 3.91$ rad/sec)

4.3.3 Curve Fit of Imaginary Part of $H(j\omega)$

The use of the algorithm of Appendix C provided the results shown in Table 4.6. As the damping was varied from 0.008 to 0.20, the errors did not in-

crease as in the previous two methods. The results

Table 4.6

PARAMETER	ESTIMATION	ACTUAL VALUE	% ERROR
ω_1	2.16994	2.16993	0.0004
ζ_1	0.00754	0.00764	1.29
ω_2	3.91038	3.91039	0.0003
ζ_2	0.01031	0.01068	3.50
mode	$\left[\begin{array}{c} 0.21535 \ / \ -359.37^\circ \\ 1 \ / \ 0^\circ \end{array} \right]$	$\left[\begin{array}{c} 0.21526 \ / \ -359.41^\circ \\ 1 \ / \ 0^\circ \end{array} \right]$	0.04M
1			0.01P
mode	$\left[\begin{array}{c} 1 \ / \ 0^\circ \\ 0.64594 \ / \ -178.87^\circ \end{array} \right]$	$\left[\begin{array}{c} 1 \ / \ 0^\circ \\ 0.64593 \ / \ -178.94^\circ \end{array} \right]$	0.002M
2			0.04P

for the various amounts of damping can be seen in Appendix D.8. The plot of error vs damping in Figure 4.13 clearly shows the superiority of this method.

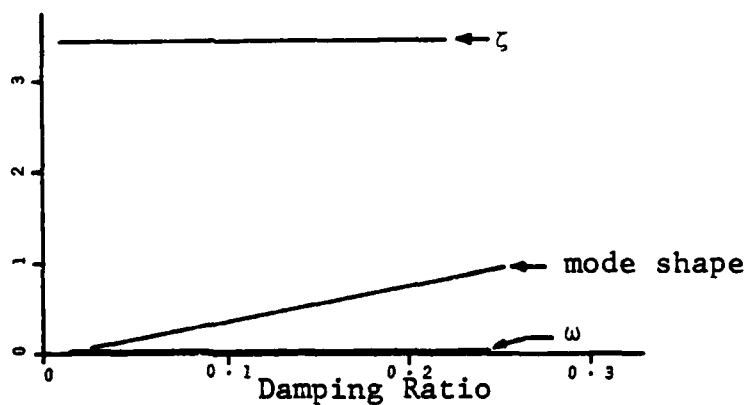


Figure 4.13. Percent Error vs Damping Ratio Using Imaginary Curve Fit, Poles Close ($\omega_1 = 2.17$ rad/sec, $\omega_2 = 3.91$ rad/sec)

Caution must be exercised in using this method and choosing the initial estimates for natural frequency and damping ratio. If the initial estimates are greater than 10% in error, as mentioned earlier, there is a possibility that the method will diverge.

4.4 Determination of Mass, Stiffness, and Damping Matrices

As an extension of example problem one, the data from Section 4.2.3, with the damping ratio approximately equal to 0.008, was used to determine the mass, stiffness, and damping matrices. This example will demonstrate the use of equations (2.21), (2.27), and (2.31).

It has been shown that the modal properties can be determined from frequency response data with relatively good accuracy (depending on the method used). The residue at each pole is measured and then used to determine the mode shape. Recall from equation (2.10) that the residue matrix for mode k can be written in terms of the normalized mode shape.

$$\underline{A}_k = a_k \underline{u}_k \underline{u}_k^T$$

Recall that the residue matrix can also be written as

AD-A091 459

AIR FORCE INST OF TECH WRIGHT-PATTERSON AFB OH F/G 12/1
DETERMINATION OF MODAL PARAMETERS FROM EXPERIMENTAL FREQUENCY R--ETC(U)
DEC 78 C W MILLER
AFIT-CI-79-182T

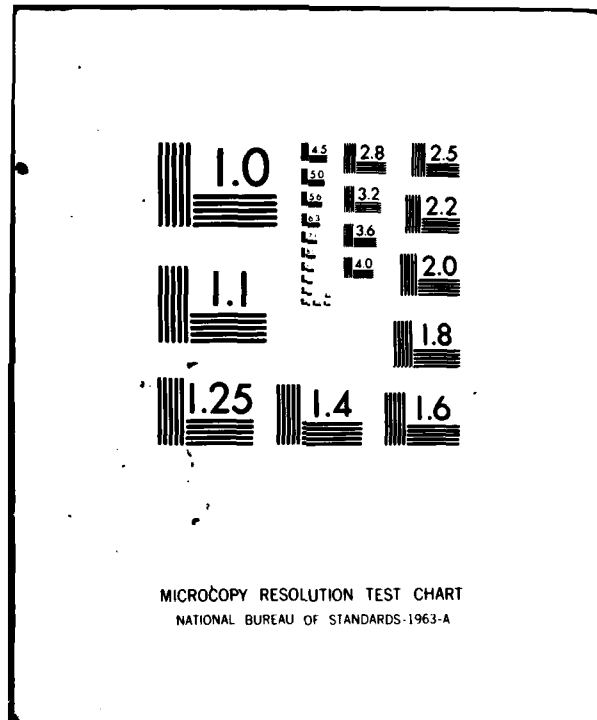
NL

UNCLASSIFIED

2
21
27

2 21 27											

END
DATE
FILMED
8-1
DTIC



MICROCOPY RESOLUTION TEST CHART
NATIONAL BUREAU OF STANDARDS-1963-A

$$A_k = \underline{r}_k \underline{r}_k^T$$

where \underline{r}_k is the measured residue vector of mode k normalized in accordance with equation (2.17). Thus

$$a_k \underline{u}_k \underline{u}_k^T = \underline{r}_k \underline{r}_k^T$$

If we again normalize the residue vector in the following manner,

$$\frac{\underline{r}_k}{\sqrt{\underline{r}_k^T \underline{r}_k}}$$

we have in essence normalized the mode shapes, i.e.

$$\frac{\underline{r}_k}{\sqrt{\underline{r}_k^T \underline{r}_k}} = \frac{\sqrt{a_k} \underline{u}_k}{\sqrt{\sqrt{a_k} \underline{u}_k^T} \sqrt{a_k \underline{u}_k^T}} = \frac{\underline{u}_k}{\sqrt{\underline{u}_k^T \underline{u}_k}}$$

Thus the normalized mode shapes needed for equations (2.21), (2.27), and (2.31) can be determined from the measured residue vectors. This normalization was performed on the measured residues. Since the residue matrix is measured and the normalized mode shapes obtained, then the complex scalars, a_k , can be determined from equation (2.10). Once the scalars are

determined, the mass, stiffness, and damping matrices may be determined using equations (2.21), (2.27), and (2.31).

After normalization, the data from Section 4.2.3 was used to predict the results tabulated in Table 4.7. From Table 4.7 it can be seen that the

Table 4.7

MATRIX	ESTIMATION	ACTUAL VALUE
<u>M</u>	$\begin{bmatrix} 1.02 & 0.00 \\ 0.00 & 6.01 \end{bmatrix}$	$\begin{bmatrix} 1.00 & 0.00 \\ 0.00 & 6.00 \end{bmatrix}$
<u>K</u>	$\begin{bmatrix} 106.84 & -6.05 \\ -6.05 & 6.01 \end{bmatrix}$	$\begin{bmatrix} 106.0 & -6.0 \\ -6.0 & 6.0 \end{bmatrix}$
<u>C</u>	$\begin{bmatrix} 0.20 & -0.10 \\ -0.10 & 0.10 \end{bmatrix}$	$\begin{bmatrix} 0.20 & -0.10 \\ -0.10 & 0.10 \end{bmatrix}$

estimations for the matrices are very good. The error in these estimations will be dependent on how well the residue matrix can be measured.

4.5 Summary

This completes the chapter on example problems. These problems have shown the limitations of each curve fit method, and also have verified equations (2.21), (2.27), and (2.31) which can be used to determine the mass, stiffness, and damping ma-

trices. The next chapter will review the results presented and draw conclusions on which curve fit method is best under given conditions.

CHAPTER V

SUMMARY AND CONCLUSIONS

Four techniques were described in Chapter III for estimating the natural frequencies, damping ratios, and mode shapes of a system using the frequency response functions measured at various points in the system. The first method discussed dealt only with the quadrature response and is only useful in very special cases. The other three techniques were investigated in more detail. The three curve fitting methods were used to solve two example problems, one with the system poles separated in frequency by approximately 10 rad/sec, and the other with the poles separated in frequency by approximately 1.7 rad/sec. These example problems pointed out the usefulness of the different techniques.

The method of Kennedy and Pancu (circle fit) provided very good estimates for natural frequencies and damping ratios, provided that the frequency resolution is adequate. However, if the mode shapes are also desired, this method begins to break down. It

was shown in Sections 4.2.1 and 4.3.1 that, when there is heavy modal overlap or when one mode dominates, the method yields large errors. For example, with the poles separated in frequency by approximately 10 rad/sec, a frequency resolution of approximately 0.02 rad/sec, and with a damping ratio of approximately 0.008, the error in the damping ratio estimate was 368%.

This was due to inadequate frequency resolution in a problem where one mode dominated. When the poles were separated by approximately 1.7 rad/sec in frequency and with the damping ratio near .20, and a frequency resolution of approximately 0.01 rad/sec, this method produced an error of 168% in the mode shape of mode 2. However, under the same conditions, the natural frequency estimations were in error by less than 3% and the damping ratios were in error by less than 8%.

It is concluded that the method of Kennedy and Pancu is reliable for estimating the natural frequencies and damping ratios except in the cases where one mode dominates or when the damping ratio exceeds 0.20.

The complex curve fit method also provided reasonable estimates under certain conditions. For instance, when the poles were separated in frequency by 10 rad/sec, with 8% damping and 0.02 rad/sec fre-

quency resolution, the errors for natural frequencies, damping ratios, and mode shapes were all less than 1%. However, with the damping at 3.8%, and the other factors as above, this method produced an error of 198% in the estimation of mode shape 2 while maintaining less than 1% error in other parameters. This large error was due to a lack of convergence (in 50 iterations) of the technique used. This method makes use of an assumption that is not valid when one mode dominates or when the degree of modal overlap is heavy. It is this assumption that causes the large errors to be generated. For example, with the poles separated in frequency by 1.7 rad/sec, damping set at 0.20, and a frequency resolution of 0.01 rad/sec, this method yielded errors in mode shapes as large as 74% and errors in natural frequencies and damping ratios as high as 16% and 88%, respectively.

It is concluded that the complex curve fit works well under the conditions of light modal overlap provided that no one mode dominates the response. When one mode dominates, the estimates are still good for the natural frequencies and damping ratios, but the estimates for the mode shapes are not reliable. When the poles are close together where they interact

to form the total response, this technique is not very reliable. The errors, again, are due primarily to poor initial estimates (computed based on an assumption that is invalid for heavy modal overlap) for which the algorithm converges to the wrong values.

A modified complex curve fit method could be investigated by using a method similar to that discussed in Section 4.2.3 to provide the initial estimates for the previously described complex curve fit. This could possibly make this method more desirable.

The final method discussed, that of curve fitting the imaginary part of the frequency response, provided excellent results for all cases considered. The maximum error for any parameter or mode shape was less than 4% for all cases considered. These cases included the poles separated in frequency by 10 rad/sec, a frequency resolution of 0.02 rad/sec, and the damping ratio varying from 0.008 to 0.20. They also included the cases where the poles were separated in frequency by 1.7 rad/sec and the frequency resolution was 0.01 rad/sec, with the damping ratio varying from 0.008 to 0.20. The results obtained using this technique makes this method the most desirable of the three methods discussed. The main problem associated

with this method is that it diverges if the initial estimates for natural frequencies and damping ratios are in error by more than 10%. Therefore caution must be used when determining the initial estimates required to start this method. It has been found that, in all cases considered, if the method converged, it did so with excellent results. Therefore, a trial and error type approach could be taken, if necessary, to determine the initial estimates. If the method diverges, then another estimate could be tried until convergence is obtained.

In summary, if only the natural frequencies and damping ratios are desired, the method of Kennedy and Pancu provides acceptable results, except where one mode is dominant. However, if the mode shapes are also desired, then the curve fit of the imaginary response is the most desirable from the standpoint of minimum error.

APPENDIX A
CIRCLE FIT ALGORITHM

```

SUBROUTINE CIRCLE(XP,YP,WP,IPLT,NDOF)
DIMENSION WP(500),XP(500),YP(500),RX(5),RI(5)
DIMENSION S(3),WN(5),X(6),Y(6),W(6),Z(5)
C THIS SUBROUTINE SEARCHES FOR THE MAXIMUM
C CHANGE IN ARC LENGTH ON THE POLAR
C PLOT OF THE FREQUENCY RESPONSE FUNCTION.
C THE FREQUENCY POINT AT WHICH THE ARC
C LENGTH IS A MAXIMUM IS DESIGNATED AS
C THE NATURAL FREQUENCY. A CIRCLE IS
C THEN FIT THROUGH FIVE POINTS; THE
C NATURAL FREQUENCY POINT AND TWO ADJ-
C ACENT POINTS ON EACH SIDE OF THE
C NATURAL FREQUENCY. TWO OTHER SUB-
C ROUTINES ARE USED TO DETERMINE THE
C MAGNITUDE AND PHASE OF THE MODE
C SHAPES AND THE DAMPING RATIOS.
C XP=THE REAL PART OF THE FREQUENCY RESPONSE
C YP=THE IMAGINARY PART OF THE FREQUENCY RESPONSE
C WP=THE FREQUENCY POINTS AT WHICH THE FREQUENCY
C RESPONSE WAS MEASURED
C IPLT=NUMBER OF POINTS IN THE FREQUENCY RESPONSE
C NDOF=THE NUMBER OF DEGREES OF FREEDOM
C S=ARC LENGTH
C WN=NATURAL FREQUENCY
C X AND Y=THE ARRAYS OF POINTS WHICH ARE USED
C FOR THE CIRCLE FIT
C Z=DAMPING RATIO
C RX AND RI=THE REAL AND IMAGINARY PART OF THE
C MODE SHAPE COMPONENT, RESPECTIVELY
IC=0
NUMPTS=IPLT-3
DO 12 I=1,NUMPTS
DO 1 J=1,3
1 S(J)=SQRT((ABS(XP(I+J)-XP(I+J-1)))**2+
$(ABS(YP(I+J)-YP(I+J-1)))**2)
IF(S(1).LT.S(2).AND.S(3).LE.S(2))GO TO 2
GO TO 10
2 IC=IC+1

```

```

IF(IC.GT.NDOF) PRINT 15
IF(S(3).GT.S(1))GO TO 4
WN(IC)=WP(I+1)
DO 3 L=1,5
W(L)=WP(I+L-2)
X(L)=XP(I+L-2)
3 Y(L)=YP(I+L-2)
GO TO 6
4 WN(IC)=WP(I+2)
DO 5 L=1,5
W(L)=WP(I+L-1)
X(L)=XP(I+L-1)
5 Y(L)=YP(I+L-1)
6 CONTINUE
CALL CIRCLE(X,Y,XCEN,YCEN,RADIUS)
PRINT 7
7 FORMAT(///,14X,*DATA POINTS*,/,5X,*OMEGA*,
$4X,*REAL PART IMAG.PART*,/)
PRINT 8,(W(L),X(L),Y(L),L=1,5)
8 FORMAT(2X,F8.4,2F12.5)
PRINT 9,XCEN,YCEN,RADIUS
9 FORMAT(///,11X,*CIRCLE PARAMETERS*,/,5X,
$*CENTER (REAL,IMAG.)*,5X,*RADIUS*,/,2X,
$*(*,F10.5,*,*,F10.5,*)*,F12.5)
IF(ABS(Y(3)).GT.ABS(YCEN)) RADIUS=-RADIUS
CALL DAMP(W,X,Y,XCEN,YCEN,RADIUS,ZETA,ALPHA)
RX(IC)=RADIUS*COS(ALPHA)*2.
RI(IC)=RADIUS*SIN(ALPHA)*2.
Z(IC)=ZETA
10 CONTINUE
IF(I.EQ.NUMPTS.AND.IC.EQ.0)PRINT 11
11 FORMAT(///,5X,*NO NATURAL FREQUENCIES*,/,
$5X,*WERE FOUND*)
12 CONTINUE
IF(IC.LT.NDOF)PRINT 16
IF(IC.EQ.0)GO TO 14
PRINT 13,(I,WN(I),RX(I),RI(I),Z(I),I=1,IC)
13 FORMAT(///,5X,*WN(*,I2,*)=*,F10.5,5X,
$*MODE SHAPE COMPONENT =(*,E13.5,*) + J(*,
$E13.5,*)*,/,5X,*DAMPING RATIO=*,F10.5)
14 CONTINUE
15 FORMAT(///,5X,*THE NUMBER OF NATURAL*,/,
$*FREQUENCIES FOUND EXCEEDS THE NUMBER*,
$/,* OF DEGREES OF FREEDOM*)
16 FORMAT(///,5X,*THE NUMBER OF NATURAL*,/,
$* FREQUENCIES FOUND IS LESS THAN THE*,/,
$* NUMBER OF DEGREES OF FREEDOM*)

```

```

RETURN
END

```

```

SUBROUTINE CIRFIT(X,Y,XCEN,YCEN,RADIUS)
DIMENSION X(5),Y(5),A(3,3),F(3),R(3)
REAL ILL
C THIS SUBROUTINE CALCULATES THE CIRCLE FIT
C PARAMETERS WHICH DETERMINE THE MAGNITUDE
C OF THE COMPLEX RESIDUE.
C THE VARIABLE ILL IS USED TO DETERMINE IF THE
C MATRIX IS ILL-CONDITIONED.
DO 1 I=1,3
DO 1 J=1,3
F(I)=0,0
1 A(I,J)=0,0
A(3,3)=5,0
DO 2 I=1,5
A(1,1)=A(1,1)+X(I)*X(I)
A(1,2)=A(1,2)+X(I)*Y(I)
A(1,3)=A(1,3)+X(I)
A(2,2)=A(2,2)+Y(I)*Y(I)
A(2,3)=A(2,3)+Y(I)
F(1)=F(1)-(X(I)*X(I)+Y(I)*Y(I))*X(I)
F(2)=F(2)-(X(I)*X(I)+Y(I)*Y(I))*Y(I)
2 F(3)=F(3)-(X(I)*X(I)+Y(I)*Y(I))
A(2,1)=A(1,2)
A(3,2)=A(2,3)
A(3,1)=A(1,3)
ILL=(A(1,1)+2.*A(1,2)+2.*A(1,3)+A(2,2)+
$2.*A(2,3)+A(3,3))/90000000.
DO 3 N=1,2
DO 3 I=N+1,3
CONST=A(I,N)/A(N,N)
IF(ABS(CONST).LE.ABS(ILL)) PRINT 6
F(I)=F(I)-F(N)*CONST
DO 3 J=N+1,3
3 A(I,J)=A(I,J)-A(N,J)*CONST
CONTINUE
R(3)=F(3)/A(3,3)
DO 5 N=1,2
M=3-N
DO 4 I=M+1,3
4 F(M)=F(M)-A(M,I)*R(I)
5 R(M)=F(M)/A(M,M)
XCEN=-R(1)/2.

```

```

        YCEN=-R(2)/2.
        RADIUS=SQRT(XCEN*XCEN+YCEN*YCEN-R(3))
6      FORMAT(1H1,5X,*THE COEFFICIENT MATRIX IS*,/,
          $5X,*ILL-CONDITIONED OR SINGULAR*,/,5X,
          $*AND THE SOLUTION MAY BE MEANINGLESS*)
        RETURN
        END

```

```

        SUBROUTINE DAMP(W,X,Y,XC,YC,R,Z,A)
        DIMENSION W(5),X(5),Y(5)
C      THIS SUBROUTINE DETERMINES THE DAMPING RATIO
C      AND THE PHASE ANGLE OF THE COMPLEX RESIDUE.
C      XC=X-COORDINATE OF THE CIRCLE CENTER
C      YC=Y-COORDINATE OF THE CIRCLE CENTER
C      R=RADIUS OF THE CIRCLE
C      Z=DAMPING RATIO
C      A=PHASE ANGLE IN RADIANS
        C1SQ=(X(3)-X(2))*(X(3)-X(2))+(Y(3)-
          $Y(2))*(Y(3)-Y(2))
        C2SQ=(X(4)-X(3))*(X(4)-X(3))+(Y(4)-
          $Y(3))*(Y(4)-Y(3))
        S1=(SQRT(C1SQ))/2.
        S2=(SQRT(C2SQ))/2.
        B1=SQRT(R**2-S1**2)
        B2=SQRT(R**2-S2**2)
        THETA1=2.*ATAN2(S1,B1)
        THETA2=2.*ATAN2(S2,B2)
        PHI1=(3.14159265-THETA1)/2.
        PHI2=(3.14159265+THETA2)/2.
        BETA1=W(2)/W(3)
        BETA2=W(4)/W(3)
        Z1=((1.-BETA1**2)*SIN(PHI1)/COS(PHI1))/
          $(2.*BETA1)
        Z2=((1.-BETA2**2)*SIN(PHI2)/COS(PHI2))/
          $(2.*BETA2)
        Z=(Z1+Z2)/2.
        XX2=ABS(X(3)-XC)
        YY2=ABS(Y(3)-YC)
        IF(Y(3).GT.YC)GO TO 1
        A=ATAN2(XX2,YY2)
        IF(X(3).LT.XC)A=-A
        GO TO 2
1      A=ATAN2(YY2,XX2)+1.57079632
        IF(X(3).LT.XC)A=-A
2      CONTINUE

```


RETURN
END

APPENDIX B

MULTI DEGREE OF FREEDOM CURVE FIT ALGORITHM

```

SUBROUTINE HJW(XP,YP,WP,IPLT,NDOF)
DIMENSION WP(500),XP(500),YP(500)
DIMENSION W1(5),W2(5),H1R(5),H1I(5)
DIMENSION H2R(5),H2I(5),WN(5),RR(5),RI(5)
DIMENSION SR(5,2),SI(5),AR(5),AI(5),Z(5)
C THIS SUBROUTINE PICKS OUT THE PEAKS IN
C THE IMAGINARY PART OF THE FREQUENCY
C RESPONSE. TWO POINTS, ONE ON EACH
C SIDE OF THE PEAK, ARE PICKED FOR
C EACH PEAK. THESE POINTS ARE THEN
C USED IN THE TWO POINT ESTIMATION
C TECHNIQUE.
C XP=REAL PART OF THE FREQUENCY RESPONSE
C YP=IMAGINARY PART OF THE FREQUENCY
C RESPONSE
C WP=FREQUENCY POINTS AT WHICH THE FRE-
C QUENCY RESPONSE WAS MEASURED
C IPLT=NUMBER OF POINTS IN THE FREQUENCY
C RESPONSE
C NDOF=NUMBER OF DEGREES OF FREEDOM
NUMPTS=IPT-2
NPEAKS=0
DO 6 I=1,NUMPTS
IF(NPEAKS.GT.NDOF) PRINT 29
IF(ABS(YP(I+1)).GE.ABS(YP(I)).AND.ABS(YP(I+
$2)).LE.ABS(YP(I+1))) GO TO 1
GO TO 4
1 NPEAKS=NPEAKS+1
DO 2 JJ=1,2
IJK=I+1-JJ
IJK=I+1+JJ
RATIO1=ABS(YP(I+1)/YP(IJK))
IF(RATIO1.GE.1.0592537)GO TO 3
2 CONTINUE
3 W1(NPEAKS)=WP(IJK)
W2(NPEAKS)=WP(IJL)
H1R(NPEAKS)=XP(IJK)
H1I(NPEAKS)=YP(IJK)

```

```

H2R(NPEAKS)=XP(IJL)
H2I(NPEAKS)=YP(IJL)
4 CONTINUE
IF(NPEAKS.EQ.0.AND.I.EQ.NUMPTS)PRINT 5
5 FORMAT(/,5X,*NO NATURAL FREQUENCIES*,/,5X,
$*WERE FOUND*)
6 CONTINUE
IF(NPEAKS.EQ.0)GO TO 28
PRINT 7,NPEAKS
7 FORMAT(1H1,5X,I2,* RESONANT FREQUENCIES*,/,
$5X,*WERE FOUND*)
PRINT 8
8 FORMAT(/,5X,*POINTS USED IN ESTIMATION*,
$/ ,7X,*(2 PER PEAK)*)
DO 9 IJ=1,NPEAKS
9 PRINT 10,IJ,H1R(IJ),H1I(IJ),IJ,H2R(IJ),H2I(IJ)
10 FORMAT(/,5X,*H1(*,I2,*)= (*,E13.5,*)+
$J(*,E13.5,*)*,/,5X,*H2(*,I2,*)= (*,
$E13.5,*)+J(*,E13.5,*)*)
DO 11 IJ=1,NPEAKS
SR(IJ,1)=0.0
RR(IJ)=0.0
11 RI(IJ)=0.0
NN=1
12 CONTINUE
DO 13 MP=1,NPEAKS
T=H1R(MP)-RR(MP)
D=H1I(MP)-RI(MP)
E=H2R(MP)-RR(MP)
F=H2I(MP)-RI(MP)
G=H1R(MP)-H2R(MP)
P=H1I(MP)-H2I(MP)
SR(MP,2)=((W2(MP)*F-W1(MP)*D)*G+(W1(MP)*T-
$W2(MP)*E)*P)/(G*G+P*P)
SI(MP)=((W1(MP)*T-W2(MP)*E)*G-(W2(MP)*F-
$W1(MP)*D)*P)/(G*G+P*P)
AR(MP)=0.5*(-(SR(MP,2)*(T+E)+D*(W1(MP)-
$SI(MP))+F*(W2(MP)-SI(MP))))
AI(MP)=0.5*(T*(W1(MP)-SI(MP))+E*(W2(MP)-
$SI(MP))-SR(MP,2)*(D+F))
13 CONTINUE
ICON=0
DO 14 JCT=1,NPEAKS
DIFF=ABS(SR(JCT,2)-SR(JCT,1))
IF(DIFF.LE..000001)ICON=ICON+1
IF(ICON.EQ.NPEAKS)GO TO 25
14 CONTINUE

```

```

RPR=0.0
RPI=0.0
IF(NN.EQ.1)GO TO 17
DO 16 I=1,IPLT
SUMR=0.0
SUMI=0.0
DO 15 J=1,NPEAKS
Z1=-2.*(AR(J)*SR(J,2)+AI(J)*SI(J))
Z2=2.*WP(I)*AR(J)
Z3=SR(J,2)*SR(J,2)+SI(J)*SI(J)-WP(I)*WP(I)
Z4=2.*WP(I)*SR(J,2)
SUMR=SUMR+((Z1*Z3-Z2*Z4)/(Z3*Z3+Z4*Z4))
SUMI=SUMI+((Z2*Z3+Z1*Z4)/(Z3*Z3+Z4*Z4))
15 CONTINUE
RPR=RPR+XP(I)-SUMR
RPI=RPI+YP(I)-SUMI
16 CONTINUE
RIPLT=FLOAT(IPLT)
RPR=RPR/RIPLT
RPI=RPI/RIPLT
17 CONTINUE
DO 21 MR=1,NPEAKS
RBR=0.0
RBI=0.0
DO 20 NR=1,2
WW=W1(MR)
IF(NR.EQ.2)WW=W2(MR)
RBCR=(-(AR(MR)*SR(MR,2))-AI(MR)*(WW+
$SI(MR)))/(SR(MR,2)*SR(MR,2)+(WW+
$SI(MR))*(WW+SI(MR)))
RBCI=(AI(MR)*SR(MR,2)-AR(MR)*(WW+
$SI(MR)))/(SR(MR,2)*SR(MR,2)+(WW+
$SI(MR))*(WW+SI(MR)))
SUMR=0.0
SUMI=0.0
IF(NPEAKS.EQ.1)TO TO 19
DO 18 KR=1,NPEAKS
IF(KR.EQ.MR)GO TO 18
Q1=-2.*(AR(KR)*SR(KR,2)+AI(KR)*SI(KR))
Q2=2.*WW*AR(KR)
Q3=SR(KR,2)*SR(KR,2)+SI(KR)*SI(KR)-WW*WW
Q4=2.*WW*SR(KR,2)
DENOM=Q3*Q3+Q4*Q4
SUMR=SUMR+((Q1*Q3-Q2*Q4)/DENOM)
SUMI=SUMI+((Q2*Q3+Q1*Q4)/DENOM)
18 CONTINUE
19 RBR=RBR+RBCR+SUMR

```

```

RBI=RBI+RBCI+SUMI
20  CONTINUE
    RBR=RBR/2.
    RBI=RBI/2.
    RR(MR)=RBR+RPR
    RI(MR)=RBI+RPI
21  CONTINUE
    DO 22 IA=1,NPEAKS
22  SR(IA,1)=SR(IA,2)
    NN=NN+1
    IF(NN.GT.50)TO TO 23
    GO TO 12
23  PRINT 24,DIFF
24  FORMAT(///,5X,*CONVERGENCE NOT OBTAINED*,
$/ ,5X,*ON THE REAL PART OF THE POLES ON*,
$/ ,5X,*ALL PEAKS IN 50 ITERATIONS*,//,5X,
$*DIFFERENCE BETWEEN LAST TWO ITERATIONS*,
$/ ,5X,*ON THE REAL PART OF THE POLES*,/,
$5X,*WAS =*,F14.6)
25  CONTINUE
    IF(NPEAKS.LT.NDOF) PRINT 30
    DO 26 LL=1,NPEAKS
    WN(LL)=SQRT(SR(LL,2)*SR(LL,2)+SI(LL)*
$SI(LL))
    Z(LL)=-SR(LL,2)/WN(LL)
26  PRINT 27,LL,WN(LL),Z(LL),AR(LL),AI(LL)
27  FORMAT(//,8X,*POLE NUMBER *,I2,/,
$3X,*NATURAL FREQUENCY =*,F10.5,5X,
$*DAMPING RATIO =*,F10.5,/,3X,
$*MODE SHAPE COMPONENT = (*,E13.5,
$*) +/- J(*,E13.5,*)*)
28  CONTINUE
29  FORMAT(1H1,3X,*THE NUMBER OF PEAKS*,/,3X,
$*EXCEEDS THE NUMBER OF DEGREES OF*,/,3X,
$*FREEDOM*)
30  FORMAT(//,3X,*THE NUMBER OF PEAKS*,/,3X,
$*IS LESS THAN THE NUMBER OF DEGREES*,/,
$3X,*OF FREEDOM*)
    RETURN
    END

```

APPENDIX C

IMAGINARY CURVE FIT ALGORITHM

```

SUBROUTINE QUAD(YP,WP,IPLT,NDOF,K,WN,Z)
DIMENSION WP(500),YP(500),F(10),U(10)
DIMENSION W1(5),W2(5),SNEW(5),W(10)
DIMENSION H3I(5),H4I(5),W3(5),W4(5)
DIMENSION H1I(5),Z(5),H2I(5),WN(5)
DIMENSION SR(5),SI(5),AR(5),AI(5)
DIMENSION ADD(4),A1(4),A2(4)
REAL JAC(5,10)
C THIS SUBROUTINE CURVE FITS THE IMAG-
C INARY PART OF THE FREQUENCY RESPONSE.
C INITIAL ESTIMATES FOR THE NATURAL
C FREQUENCIES AND DAMPING RATIOS
C MUST BE INPUT.
C YP=IMAGINARY PART OF THE FREQUENCY
C RESPONSE
C WP=FREQUENCY POINTS AT WHICH THE
C RESPONSE IS MEASURED
C IPLT=NUMBER OF POINTS IN THE
C RESPONSE
C NDOF=NUMBER OF DEGREES OF FREEDOM
C K=NUMBER OF INITIAL ESTIMATES THAT
C ARE INPUT
C WN=INITIAL ESTIMATES FOR NATURAL
C FREQUENCIES
C Z=INITIAL ESTIMATES FOR THE DAMPING
C RATIOS
NUMPTS=IPLT-2
NPEAKS=0
DO 4 I=1,NUMPTS
IF(NPEAKS.GT.NDOF)PRINT 21
IF(ABS(YP(I+1)).GE.ABS(YP(I)).AND.ABS(YP(I+
$2)).LE.ABS(YP(I+1)))GO TO 1
GO TO 2
1 NPEAKS=NPEAKS+1
W1(NPEAKS)=WP(I-7)
W2(NPEAKS)=WP(I+9)
H1I(NPEAKS)=YP(I-7)
H2I(NPEAKS)=YP(I+9)

```

```

W3(NPEAKS)=WP(I-13)
W4(NPEAKS)=WP(I+15)
H3I(NPEAKS)=YP(I-13)
H4I(NPEAKS)=YP(I+15)
WN(NPEAKS)=WP(I+1)
2 CONTINUE
IF(NPEAKS.EQ.0.AND.I.EQ.NUMPTS)PRINT 3
3 FORMAT(//,5X,*NO RESONANT FREQUENCIES*,
$1X,*WERE FOUND*)
4 CONTINUE
IF(NPEAKS.EQ.0)GO TO 22
IF(NPEAKS.LT.NDOF) PRINT 5
5 FORMAT(1H1,5X,*THE NUMBER OF PEAKS*,
$1X,*FOUND IS LESS THAN THE NUMBER*,
$1X,*OR DEGREES OF FREEDOM*)
DO 6 I=1,K
SR(I)=-Z(I)*WN(I)
6 SI(I)=WN(I)*SQRT(1.-Z(I)*Z(I))
DO 7 MP=1,NPEAKS
IN=2*MP
W(IN-1)=W1(MP)
W(IN)=W2(MP)
F(IN-1)=H1I(MP)
7 F(IN)=H2I(MP)
CALL GAUSS(SR,SI,NPEAKS,W,F,U)
DO 8 MP=1,NPEAKS
IN=2*MP
SNEW(MP)=0.0
AR(MP)=U(IN-1)
8 AI(MP)=U(IN)
PRINT 9
9 FORMAT(1H1,3X,*INITIAL VALUES*,//)
DO 10 MP=1,NPEAKS
10 PRINT 11,MP,WN(MP),Z(MP),AR(MP),AI(MP)
11 FORMAT(6X,*POLE NO.*,I2,/,2X,
$*NATURAL FREQUENCY=*,F10.5,5X,
$*DAMPING RATIO=*,F10.5,/,2X,
$*RESIDUE VECTOR= (*,E13.5,
$*) */- J(*,E13.5,*)*)
NN=1
12 CONTINUE
DO 16 I=1,NPEAKS
DO 15 NR=1,4
WW=W1(I)
IF(NR.EQ.2)WW=W2(I)
IF(NR.EQ.3)WW=W3(I)
IF(NR.EQ.4)WW=W4(I)

```

```

ADD(NR)=0.
DO 14 KR=1,NPEAKS
Q1=(2.*AR(KR)*SI(KR)*SI(KR)-
$2.*AR(KR)*WW*WW-2.*SR(KR)*SR(KR)*
$AR(KR)-4.*AR(KR)*SI(KR)*AI(KR))*WW
Q2=(SR(KR)*SR(KR)+2.*SI(KR)*SI(KR)+
$2.*WW*WW)*(SR(KR)*SR(KR))+(SI(KR)*
$SI(KR))*(SI(KR)*SI(KR)-2.*WW*WW)+WW**4
IF(NPEAKS.EQ.1)GO TO 13
IF(KR.EQ.1)GO TO 13
ADD(NR)=ADD(NR)+Q1/Q2
GO TO 14
13 Z1(NR)=Q1
Z2(NR)=Q2
14 CONTINUE
JAC(NR,1)=(Z2(NR)*(-4.*SR(I)*AR(I)*WW-
$4.*SI(I)*AI(I)*WW)-Z1(NR)*(4.*(SR(I)*
$SR(I)*SR(I)+4.*SR(I)*SI(I)*SI(I)+4.*
$SR(I)*WW*WW))/(Z2(NR)*Z2(NR))
JAC(NR,2)=(Z2(NR)*(4.*WW*AR(I)*SI(I)-
$4.*WW*SR(I)*AI(I))-Z1(NR)*(4.*SR(I)*
$SR(I)*SI(I)+4.*SI(I)*SI(I)*SI(I)-
$4.*SI(I)*WW*WW))/(Z2(NR)*Z2(NR))
JAC(NR,3)=(2.*WW*(SI(I)*SI(I)-WW*WW-
$SR(I)*SR(I)))/Z2(NR)
JAC(NR,4)=-4.*SR(I)*SI(I)*WW/Z2(NR)
15 CONTINUE
G1=Z1(1)/Z2(1)+ADD(1)-H1I(I)
G2=Z1(2)/Z2(2)+ADD(2)-H2I(I)
G3=Z1(3)/Z2(3)+ADD(3)-H3I(I)
G4=Z1(4)/Z2(4)+ADD(4)-H4I(I)
ISIZE=4
CALL INVERT(JAC,DMT,ISIZE,15,5)
SR(I)=SR(I)=(JAC(1,1)*G1+JAC(1,2)*G2+
$JAC(1,3)*G3+JAC(1,4)*G4)
SI(I)=SI(I)-(JAC(2,1)*G1+JAC(2,2)*G2+
$JAC(2,3)*G3+JAC(2,4)*G4)
AR(I)=AR(I)-(JAC(3,1)*G1+JAC(3,2)*G2+
$JAC(3,3)*G3+JAC(3,4)*G4)
AI(I)=AI(I)-(JAC(4,1)*G1+JAC(4,2)*G2+
$JAC(4,3)*G3+JAC(4,4)*G4)
16 CONTINUE
ICON=0
DO 17 J=1,NPEAKS
DIFF=ABS(SR(J)-SNEW(J))
IF(DIFF.LE..000001)ICON=ICON+1
IF(ICON.EQ.NPEAKS)GO TO 18

```



```

17  SNEW(J)=SR(J)
    NN=NN+1
    IF(NN.GT.50)GO TO 18
    GO TO 12
18  CONTINUE
    PRINT 19
19  FORMAT(///// ,3X,*FINAL VALUES*,//)
    DO 20 I=1,NPEAKS
    WN(I)=SQRT(SR(I)*SR(I)+SI(I)*SI(I))
    Z(I)=-SR(I)/WN(I)
20  PRINT 11,I,WN(I),Z(I),AR(I),AI(I)
21  FORMAT(1H1,3X,*THE NUMBER OF PEAKS*,
    $1X,*FOUND EXCEEDS THE NUMBER OF*,
    $1X,*DEGREES OF FREEDOM*)
22  CONTINUE
    RETURN
    END

```

```

SUBROUTINE INVERT(A,DET,N,NDIGIT,NDIM)
DIMENSION A(NDIM,8)
C THIS SUBROUTINE INVERTS A MATRIX
C AND CALCULATES THE DETERMINANT.
SUM=0.
DO 1 I=1,N
DO 1 J=1,N
1 SUM=SUM+ABS(A(I,J))
SUM=10.**(-NDIGIT/2.)*SUM/N**2
NPN=N+1
NPN=N+N
DO 2 I=1,N
IPN=1+N
DO 2 J=NPN,NPN
A(I,J)=0.
2 IF(IPN.EQ.J) A(I,J)=1.
DET=1.
INTCH=0
DO 9 I=1,N
IP1=I+1
IF(I.EQ.N) GO TO 5
M=I
DO 3 J=IP1,N
3 IF(ABS(A(M,I)).LT.ABS(A(J,I)))M=J
IF(M.EQ.I) GO TO 5
INTCH=INTCH+1
DO 4 J=1,NPN

```

```

TEMP=A(M,J)
A(M,J)=A(I,J)
4 A(I,J)=TEMP
5 IF(A(I,I).EQ.0.) GO TO 11
IF(ABS(A(I,I)).LT.SUM) PRINT 15
DO 6 J=IP1,NPN
6 A(I,J)=A(I,J)/A(I,I)
DO 8 J=1,N
IF(J.EQ.1) GO TO 8
DO 7 K=IP1,NPN
7 A(J,K)=A(J,K)-A(J,I)*A(I,K)
A(J,I)=0.
8 CONTINUE
9 DET=DET*A(I,I)
DET=(-1)**INTCH*DET
DO 10 I=1,N
DO 10 J=1,N
10 A(I,J)=A(I,J+N)
GO TO 13
11 PRINT 14
DO 12 I=1,N
DO 12 J=1,N
12 A(I,J)=1.
13 CONTINUE
14 FORMAT(/,10X,*THE MATRIX IS SINGULAR*,
$1X,*AND THEREFORE NO INVERSE EXISTS*,
$/,10X,*THE ELEMENTS OF THE MATRIX*,1X,
$*ARE ARBITRARILY SET TO 1*,/)
15 FORMAT(/,10X,*THE MATRIX IS ILL-CONDI*,
$*TIONED OR SINGULAR AND THE SOLUTION*,
$1X,*MAY BE MEANINGLESS*,/)
RETURN
END

```

```

SUBROUTINE GAUSS(X,Y,M,W,F,U)
DIMENSION X(1),Y(1),W(1),F(1),U(1),D(10,10)
N2=2*M
DO 1 N=1,M
I=2*N
DO 1 K=1,N2
TOP1=2,*W(K)*(Y(N)*Y(N)-X(N)*X(N)-
$W(K)*W(K))
TOP2=-4.*W(K)*X(N)*Y(N)
BOT=(X(N)*X(N))**2+(Y(N)*Y(N))**2+
$(W(K)*W(K))**2+2.*X(N)*X(N)*Y(N)*

```

```
SY(N)+2.*W(K)*W(K)*(X(N)*X(N)-
SY(N)*Y(N))
D(K,I-1)=TOP1/BOT
D(K,I)=TOP2/BOT
1 CONTINUE
N3=N2-1
DO 3 N=1,N3
DO 3 I=N+1,N3
CONST=D(I,N)/D(N,N)
IF(ABS(CONST).LE..0000000001)PRINT 2
2 FORMAT(/,3X,*THE D-MATRIX IS ILL-CONDI*,
$*TIONED*)
F(I)=F(I)-F(N)*CONST
DO 3 J=N+1,N2
D(I,J)=D(I,J)-D(N,J)*CONST
3 CONTINUE
U(N2)=F(N2)/D(N2,N2)
DO 5 NI=1,N3
N=N2-NI
DO 4 I=N+1,N2
4 F(N)=F(N)-D(N,I)*U(I)
5 U(N)=F(N)/D(N,N)
RETURN
END
```

APPENDIX D

DATA

D.1 Exact Solutions - Poles Separated

MULTIPLIER OF DAMPING MATRIX = 1	
PARAMETER	ACTUAL VALUE
ω_1	0.97103
ζ_1	0.00765
ω_2	10.29834
ζ_2	0.00980
mode 1	$\begin{bmatrix} 0.05711 & \angle -359.17 \\ 1 & 0 \end{bmatrix}$
mode 2	$\begin{bmatrix} 1 & 0 \\ 0.00964 & \angle -171.27 \end{bmatrix}$

MULTIPLIER OF DAMPING MATRIX = 5	
PARAMETER	ACTUAL VALUE
ω_1	0.97118
ζ_1	0.03827
ω_2	10.29677
ζ_2	0.04900
mode 1	$\begin{bmatrix} 0.05714 & \angle -355.85 \\ 1 & 0 \end{bmatrix}$
mode 2	$\begin{bmatrix} 1 & 0 \\ 0.01225 & \angle -143.37 \end{bmatrix}$

MULTIPLIER OF DAMPING MATRIX = 10	
PARAMETER	ACTUAL VALUE
ω_1	0.97164
ζ_1	0.07657
ω_2	10.29186
ζ_2	0.09803
mode 1	$\begin{bmatrix} 0.05711 & /-351.70 \\ 1 & / 0 \end{bmatrix}$
mode 2	$\begin{bmatrix} 1 & / 0 \\ 0.01812 & /-126.40 \end{bmatrix}$

MULTIPLIER OF DAMPING MATRIX = 15	
PARAMETER	ACTUAL VALUE
ω_1	0.97242
ζ_1	0.11493
ω_2	10.28362
ζ_2	0.14715
mode 1	$\begin{bmatrix} 0.05735 & /-347.52 \\ 1 & / 0 \end{bmatrix}$
mode 2	$\begin{bmatrix} 1 & / 0 \\ 0.02507 & /-119.42 \end{bmatrix}$

MULTIPLIER OF DAMPING MATRIX = 20	
PARAMETER	ACTUAL VALUE
ω_1	0.97352
ζ_1	0.15338
ω_2	10.27200
ζ_2	0.19639
mode 1	$\begin{bmatrix} 0.05755 & /-343.30 \\ 1 & / 0 \end{bmatrix}$
mode 2	$\begin{bmatrix} 1 & / 0 \\ 0.03245 & /-116.59 \end{bmatrix}$

D.2 Circle Fit Data - Poles Separated

MULTIPLIER OF DAMPING MATRIX = 1		
PARAMETER	ESTIMATION	% ERROR
ω_1	0.96000	1.14
ζ_1	0.03577	367.58
ω_2	10.29800	0.003
ζ_2	0.00980	0.0
mode 1	$\left[\begin{array}{l} 0.05711 \ / \ -359.16 \\ 1 \ / \ 0 \end{array} \right]$	0.0M* 0.003P
mode 2	$\left[\begin{array}{l} 1 \ / \ 0 \\ 0.00965 \ / \ -171.26 \end{array} \right]$	0.11M 0.01P

*M = Magnitude, P = Phase

MULTIPLIER OF DAMPING MATRIX = 5		
PARAMETER	ESTIMATION	% ERROR
ω_1	0.96000	1.15
ζ_1	0.04185	9.35
ω_2	10.27500	0.21
ζ_2	0.04915	0.31
mode 1	$\left[\begin{array}{l} 0.05704 \ / \ -355.81 \\ 1 \ / \ 0 \end{array} \right]$	0.17M 0.01P
mode 2	$\left[\begin{array}{l} 1 \ / \ 0 \\ 0.01247 \ / \ -143.50 \end{array} \right]$	1.81M 0.09P

MULTIPLIER OF DAMPING MATRIX = 10		
PARAMETER	ESTIMATION	% ERROR
ω_1	0.96000	1.20
ζ_1	0.07859	2.64
ω_2	10.25200	0.38
ζ_2	0.07866	0.64
mode 1	$\begin{bmatrix} 0.05704 & /-351.45 \\ 1 & / 0 \end{bmatrix}$	0.32M 0.07M
mode 2	$\begin{bmatrix} 1 & / 0 \\ 0.01906 & /-126.80 \end{bmatrix}$	5.21M 0.32P

MULTIPLIER OF DAMPING MATRIX = 15		
PARAMETER	ESTIMATION	% ERROR
ω_1	0.96000	1.28
ζ_1	0.11709	1.84
ω_2	10.16000	1.20
ζ_2	0.14975	1.77
mode 1	$\begin{bmatrix} 0.05730 & /-346.93 \\ 1 & / 0 \end{bmatrix}$	0.11M 0.17P
mode 2	$\begin{bmatrix} 1 & / 0 \\ 0.02734 & /-121.64 \end{bmatrix}$	9.07M 1.86P

MULTIPLIER OF DAMPING MATRIX = 20		
PARAMETER	ESTIMATION	% ERROR
ω_1	0.96000	1.39
ζ_1	0.15752	2.70
ω_2	10.06800	1.99
ζ_2	0.20226	2.99
mode 1	$\begin{bmatrix} 0.05819 & /-341.72 \\ 1 & / 0 \end{bmatrix}$	1.12M 0.46P
mode 2	$\begin{bmatrix} 1 & / 0 \\ 0.03767 & /-117.24 \end{bmatrix}$	16.09M 0.55P

D.3 Complex Curve Fit - Poles Separated

MULTIPLIER OF DAMPING MATRIX = 1		
PARAMETER	ESTIMATION	% ERROR
ω_1	0.97103	0.0
ζ_1	0.00765	0.0
ω_2	10.29834	0.0
ζ_2	0.00980	0.0
mode 1	$\left[\begin{array}{c} 0.05712 \ / \ -359.17 \\ 1 \ / \ 0 \end{array} \right]$	0.02M 0.0P
mode 2	$\left[\begin{array}{c} 1 \ / \ 0 \\ 0.01243 \ / \ -176.35 \end{array} \right]$	28.94M* 2.97P

*Convergence not obtained in 50 iterations

MULTIPLIER OF DAMPING MATRIX = 5		
PARAMETER	ESTIMATION	% ERROR
ω_1	0.97120	0.002
ζ_1	0.03829	0.05
ω_2	10.29683	0.001
ζ_2	0.04896	0.08
mode 1	$\left[\begin{array}{c} 0.05716 \ / \ -355.83 \\ 1 \ / \ 0 \end{array} \right]$	0.03M 0.01P
mode 2	$\left[\begin{array}{c} 1 \ / \ 0 \\ 0.03657 \ / \ -147.07 \end{array} \right]$	198.49M* 2.58P

*Convergence not obtained in 50 iterations

MULTIPLIER OF DAMPING MATRIX = 10		
PARAMETER	ESTIMATION	% ERROR
ω_1	0.97201	0.04
ζ_1	0.07664	0.09
ω_2	10.29230	0.004
ζ_2	0.09778	0.26
mode 1	$\begin{bmatrix} 0.05723 & /-352.06 \\ 1 & / 0 \end{bmatrix}$	0.02M 0.10P
mode 2	$\begin{bmatrix} 1 & / 0 \\ 0.01822 & /-127.40 \end{bmatrix}$	0.56M 0.79P

MULTIPLIER OF DAMPING MATRIX = 15		
PARAMETER	ESTIMATION	% ERROR
ω_1	0.97446	0.21
ζ_1	0.11491	0.02
ω_2	10.28629	0.03
ζ_2	0.14631	0.57
mode 1	$\begin{bmatrix} 0.05723 & /-348.86 \\ 1 & / 0 \end{bmatrix}$	0.23M 0.39P
mode 2	$\begin{bmatrix} 1 & / 0 \\ 0.02607 & /-121.32 \end{bmatrix}$	3.99M 1.59P

MULTIPLIER OF DAMPING MATRIX = 20		
PARAMETER	ESTIMATION	% ERROR
ω_1	0.98066	0.73
ζ_1	0.15382	0.29
ω_2	10.28007	0.08
ζ_2	0.19437	1.03
mode 1	$\begin{bmatrix} 0.05731 & /-346.91 \\ 1 & / 0 \end{bmatrix}$	0.42M 1.05P
mode 2	$\begin{bmatrix} 1 & / 0 \\ 0.03573 & /-118.49 \end{bmatrix}$	10.11M 1.63P

D.4 Imaginary Curve Fit - Poles Separated

MULTIPLIER OF DAMPING MATRIX = 1		
PARAMETER	ESTIMATION	% ERROR
ω_1	0.97103	0.0
ζ_1	0.00765	0.0
ω_2	10.29834	0.0
ζ_2	0.00980	0.0
mode 1	$\begin{bmatrix} 0.05712 & /-359.17 \\ 1 & / 0 \end{bmatrix}$	0.01M 0.0P
mode 2	$\begin{bmatrix} 1 & / 0 \\ 0.00964 & /-171.29 \end{bmatrix}$	0.0M 0.01P

MULTIPLIER OF DAMPING MATRIX = 5		
PARAMETER	ESTIMATION	% ERROR
ω_1	0.97118	0.0
ζ_1	0.03827	0.0
ω_2	10.29677	0.0
ζ_2	0.04900	0.0
mode 1	$\begin{bmatrix} 0.05715 & /-355.86 \\ 1 & / 0 \end{bmatrix}$	0.02M 0.003P
mode 2	$\begin{bmatrix} 1 & / 0 \\ 0.01224 & /-143.39 \end{bmatrix}$	0.06M 0.01P

MULTIPLIER OF DAMPING MATRIX = 10		
PARAMETER	ESTIMATION	% ERROR
ω_1	0.97164	0.0
ζ_1	0.07657	0.0
ω_2	10.29186	0.0
ζ_2	0.09803	0.0
mode 1	$\begin{bmatrix} 0.05722 & /-351.70 \\ 1 & / 0 \end{bmatrix}$	0.0M 0.0P
mode 2	$\begin{bmatrix} 1 & / 0 \\ 0.01812 & /-126.4 \end{bmatrix}$	0.0M 0.0P

MULTIPLIER OF DAMPING MATRIX = 15		
PARAMETER	ESTIMATION	% ERROR
ω_1	0.97242	0.0
ζ_1	0.11493	0.0
ω_2	10.28362	0.0
ζ_2	0.14715	0.0
mode 1	$\begin{bmatrix} 0.05735 & /-347.52 \\ 1 & / 0 \end{bmatrix}$	0.02M 0.0P
mode 2	$\begin{bmatrix} 1 & / 0 \\ 0.02507 & /-119.42 \end{bmatrix}$	0.0M 0.0P

MULTIPLIER OF DAMPING MATRIX = 20		
PARAMETER	ESTIMATION	% ERROR
ω_1	0.97352	0.0
ζ_1	0.15338	0.0
ω_2	10.27200	0.0
ζ_2	0.19639	0.0
mode 1	$\begin{bmatrix} 0.05754 & /-343.30 \\ 1 & / 0 \end{bmatrix}$	0.02M 0.0P
mode 2	$\begin{bmatrix} 1 & / 0 \\ 0.03245 & /-116.58 \end{bmatrix}$	0.0M 0.01P

D.5 Exact Solutions - Poles Close

MULTIPLIER OF DAMPING MATRIX = 1	
PARAMETER	ACTUAL VALUE
ω_1	2.16993
ζ_1	0.00764
ω_2	3.91039
ζ_2	0.01068
mode 1	$\begin{bmatrix} 0.21526 & /-359.41 \\ 1 & / 0 \end{bmatrix}$
mode 2	$\begin{bmatrix} 1 & / 0 \\ 0.64593 & /-178.94 \end{bmatrix}$

MULTIPLIER OF DAMPING MATRIX = 5	
PARAMETER	ACTUAL VALUE
ω_1	2.17059
ζ_1	0.03817
ω_2	3.90920
ζ_2	0.05342
mode 1	$\begin{bmatrix} 0.21561 & /-357.06 \\ 1 & / 0 \end{bmatrix}$
mode 2	$\begin{bmatrix} 1 & / 0 \\ 0.65020 & /-174.73 \end{bmatrix}$

MULTIPLIER OF DAMPING MATRIX = 10	
PARAMETER	ACTUAL VALUE
ω_1	2.17268
ζ_1	0.07632
ω_2	3.90545
ζ_2	0.10691
mode 1	$\begin{bmatrix} 0.21671 & /-354.12 \\ 1 & / 0 \end{bmatrix}$
mode 2	$\begin{bmatrix} 1 & / 0 \\ 0.66355 & /-169.59 \end{bmatrix}$
MULTIPLIER OF DAMPING MATRIX = 15	
PARAMETER	ACTUAL VALUE
ω_1	2.17620
ζ_1	0.11441
ω_2	3.89913
ζ_2	0.16055
mode 1	$\begin{bmatrix} 0.21858 & /-351.19 \\ 1 & / 0 \end{bmatrix}$
mode 2	$\begin{bmatrix} 1 & / 0 \\ 0.68580 & /-164.70 \end{bmatrix}$
MULTIPLIER OF DAMPING MATRIX = 20	
PARAMETER	ACTUAL VALUE
ω_1	2.18126
ζ_1	0.15241
ω_2	3.89009
ζ_2	0.21445
mode 1	$\begin{bmatrix} 0.22128 & /-348.25 \\ 1 & / 0 \end{bmatrix}$
mode 2	$\begin{bmatrix} 1 & / 0 \\ 0.71703 & /-160.16 \end{bmatrix}$

D.6 Circle Fit Data - Poles Close

MULTIPLIER OF DAMPING MATRIX = 1		
PARAMETER	ESTIMATION	% ERROR
ω_1	2.17000	0.003
ζ_1	0.00763	0.13
ω_2	3.91000	0.01
ζ_2	0.01068	0.0
mode 1	$\left[\begin{array}{c} 0.21510 \\ 1 \end{array} \begin{array}{c} /-359.41 \\ 0 \end{array} \right]$	0.07M 0.0P
mode 2	$\left[\begin{array}{c} 1 \\ 0.64733 \end{array} \begin{array}{c} / 0 \\ /-178.94 \end{array} \right]$	0.22M 0.0P

MULTIPLIER OF DAMPING MATRIX = 5		
PARAMETER	ESTIMATION	% ERROR
ω_1	2.17000	0.03
ζ_1	0.03791	0.68
ω_2	3.90000	0.24
ζ_2	0.05342	0.0
mode 1	$\left[\begin{array}{c} 0.21187 \\ 1 \end{array} \begin{array}{c} /-356.90 \\ 0 \end{array} \right]$	1.73M 0.24P
mode 2	$\left[\begin{array}{c} 1 \\ 0.68593 \end{array} \begin{array}{c} / 0 \\ /-174.64 \end{array} \right]$	5.50M 0.05P

MULTIPLIER OF DAMPING MATRIX = 10		
PARAMETER	ESTIMATION	% ERROR
ω_1	2.16000	0.58
ζ_1	0.07550	1.07
ω_2	3.89000	0.40
ζ_2	0.10655	0.34
mode 1	$\begin{bmatrix} 0.20627 & /-345.76 \\ 1 & / 0 \end{bmatrix}$	4.82M 2.36P
mode 2	$\begin{bmatrix} 1 & / 0 \\ 0.81231 & /-163.31 \end{bmatrix}$	22.42M 3.70P

MULTIPLIER OF DAMPING MATRIX = 15		
PARAMETER	ESTIMATION	% ERROR
ω_1	2.15000	1.20
ζ_1	0.11490	0.43
ω_2	3.87000	0.75
ζ_2	0.16058	0.02
mode 1	$\begin{bmatrix} 0.20783 & /-342.45 \\ 1 & / 0 \end{bmatrix}$	4.92M 2.49P
mode 2	$\begin{bmatrix} 1 & / 0 \\ 1.07109 & /-146.86 \end{bmatrix}$	56.18M 10.83P

MULTIPLIER OF DAMPING MATRIX = 20		
PARAMETER	ESTIMATION	% ERROR
ω_1	2.12000	2.81
ζ_1	0.16451	7.94
ω_2	3.85000	1.03
ζ_2	0.21882	2.04
mode 1	$\begin{bmatrix} 0.22771 & /-327.32 \\ 1 & / 0 \end{bmatrix}$	2.91M 6.01P
mode 2	$\begin{bmatrix} 1 & / 0 \\ 1.92458 & / 60.96 \end{bmatrix}$	168.41M 69.50P

D.7 Complex Curve Fit - Poles Close

MULTIPLIER OF DAMPING MATRIX = 1		
PARAMETER	ESTIMATION	% ERROR
ω_1	2.16993	0.0
ζ_1	0.00764	0.0
ω_2	3.91038	0.0002
ζ_2	0.01068	0.0
mode 1	$\left[\begin{array}{c} 0.21533 \ / \ -359.41 \\ 1 \ / \ 0 \end{array} \right]$	0.03M 0.0P
mode 2	$\left[\begin{array}{c} 1 \ / \ 0 \\ 0.64532 \ / \ -178.95 \end{array} \right]$	0.09M 0.01P

MULTIPLIER OF DAMPING MATRIX = 5		
PARAMETER	ESTIMATION	% ERROR
ω_1	2.17085	0.01
ζ_1	0.03852	0.92
ω_2	3.90897	0.01
ζ_2	0.05360	0.34
mode 1	$\left[\begin{array}{c} 0.21785 \ / \ -357.22 \\ 1 \ / \ 0 \end{array} \right]$	1.04M 0.04P
mode 2	$\left[\begin{array}{c} 1 \ / \ 0 \\ 0.63044 \ / \ -175.32 \end{array} \right]$	3.04M 0.34P

MULTIPLIER OF DAMPING MATRIX = 10		
PARAMETER	ESTIMATION	% ERROR
ω_1	2.17692	0.20
ζ_1	0.07954	4.22
ω_2	3.89989	0.14
ζ_2	0.10900	1.96
mode 1	$\begin{bmatrix} 0.22868 & /-355.73 \\ 1 & / 0 \end{bmatrix}$	5.52M 0.46P
mode 2	$\begin{bmatrix} 1 & / 0 \\ 0.57717 & /-175.36 \end{bmatrix}$	13.02M 3.40P

MULTIPLIER OF DAMPING MATRIX = 15		
PARAMETER	ESTIMATION	% ERROR
ω_1	2.19491	0.86
ζ_1	0.13419	17.29
ω_2	3.83325	1.69
ζ_2	0.17129	6.69
mode 1	$\begin{bmatrix} 0.27998 & /-356.02 \\ 1 & / 0 \end{bmatrix}$	28.09M 1.38P
mode 2	$\begin{bmatrix} 1 & / 0 \\ 0.52214 & /-165.29 \end{bmatrix}$	23.86M 0.36P

MULTIPLIER OF DAMPING MATRIX = 20		
PARAMETER	ESTIMATION	% ERROR
ω_1	2.52032	15.54
ζ_1	0.12580	17.46
ω_2	4.00429	2.94
ζ_2	0.40395	88.36
mode 1	$\begin{bmatrix} 0.27337 & / 269.06 \\ 1 & / 0 \end{bmatrix}$	23.54M 73.89P
mode 2	$\begin{bmatrix} 1 & / 0 \\ 0.20754 & / 117.58 \end{bmatrix}$	71.06M 41.16P

D.8 Imaginary Curve Fit - Poles Close

MULTIPLIER OF DAMPING MATRIX = 1		
PARAMETER	ESTIMATION	% ERROR
ω_1	2.16994	0.0004
ζ_1	0.00754	1.29
ω_2	3.91038	0.0003
ζ_2	0.01031	3.50
mode	$\begin{bmatrix} 0.21535 & /-359.37 \\ 1 & / 0 \end{bmatrix}$	0.04M
1		0.01P
mode	$\begin{bmatrix} 1 & / 0 \\ 0.64594 & /-178.87 \end{bmatrix}$	0.002M
2		0.04P

MULTIPLIER OF DAMPING MATRIX = 5		
PARAMETER	ESTIMATION	% ERROR
ω_1	2.17069	0.005
ζ_1	0.03770	1.22
ω_2	3.90902	0.004
ζ_2	0.05154	3.51
mode	$\begin{bmatrix} 0.21563 & /-356.87 \\ 1 & / 0 \end{bmatrix}$	0.01M
1		0.05P
mode	$\begin{bmatrix} 1 & / 0 \\ 0.65047 & /-174.38 \end{bmatrix}$	0.04M
2		0.20P

MULTIPLIER OF DAMPING MATRIX = 10		
PARAMETER	ESTIMATION	% ERROR
ω_1	2.17306	0.02
ζ_1	0.07538	1.23
ω_2	3.90476	0.02
ζ_2	0.10317	3.50
mode 1	$\begin{bmatrix} 0.21677 & /-353.73 \\ 1 & / 0 \end{bmatrix}$	0.03M 0.11P
mode 2	$\begin{bmatrix} 1 & / 0 \\ 0.66462 & /-168.90 \end{bmatrix}$	0.16M 0.41P

MULTIPLIER OF DAMPING MATRIX = 15		
PARAMETER	ESTIMATION	% ERROR
ω_1	2.17708	0.04
ζ_1	0.11301	1.23
ω_2	3.89756	0.04
ζ_2	0.15496	3.48
mode 1	$\begin{bmatrix} 0.21872 & /-350.59 \\ 1 & / 0 \end{bmatrix}$	0.07M 0.17P
mode 2	$\begin{bmatrix} 1 & / 0 \\ 0.68820 & /-163.69 \end{bmatrix}$	0.35M 0.61P

MULTIPLIER OF DAMPING MATRIX = 20		
PARAMETER	ESTIMATION	% ERROR
ω_1	2.18285	0.07
ζ_1	0.15055	1.22
ω_2	3.88725	0.07
ζ_2	0.20701	3.47
mode 1	$\begin{bmatrix} 0.22154 & /-347.45 \\ 1 & / 0 \end{bmatrix}$	0.12M 0.23P
mode 2	$\begin{bmatrix} 1 & / 0 \\ 0.72128 & /-158.84 \end{bmatrix}$	0.59M 0.82P

BIBLIOGRAPHY

1. Brooks, R. O., "Transient Response of Linear Undamped and Lightly Damped Lumped Spring-Mass Systems by Graphical Techniques," Thesis, Department of Mechanical Engineering, University of New Mexico, 1963.
2. Chestnut, H. and Mayer, R. W., Servomechanisms and Regulating System Design, John Wiley and Sons, New York, Vol. I, 1951, Vol II, 1955.
3. Crafton, P. A., Shock and Vibration in Linear Systems, Harper and Brothers, New York, 1961.
4. Hasz, J. R., "Determination of the Structural Dynamic Flexibility Matrix," Thesis, Department of Mechanical Engineering, University of Cincinnati, 1968.
5. Jacobsen, L. S. and Ayre, R. S., Engineering Vibrations, McGraw-Hill, New York, 1958.
6. Kennedy, C. C. and Pancu, C. D. P., "Use of Vectors in Vibration Measurement and Analysis," Journal of the Aeronautical Sciences, Vol. 14, November 1947.
7. Klosterman, A. L., "Determination of Dynamic Information by Use of Vector Components of Vibration," Masters Thesis, University of Cincinnati, 1968.
8. Klosterman, A. L., "On the Experimental Determination and Use of Modal Representations of Dynamic Characteristics," PhD Dissertation, University of Cincinnati, 1971.
9. Potter, R., and Richardson, M., "Mass, Stiffness, and Damping Matrices from Measured Modal Parameters," I. S. A. Conference and Exhibit, New York City, October, 1974.

10. Ramsey, K. A., "Effective Measurements for Structural Dynamics Testing," Sound and Vibration, November 1975, pages 24-35.
11. Richardson, M., "Modal Analysis Using Digital Test Systems," Seminar on Understanding Digital Control and Analysis in Vibration Test Systems, Shock and Vibration Information Center Publications, May 1975.
12. Richardson, M. and Potter, R., "Identification of Modal Properties of an Elastic Structure from Measured Transfer Function Data," 20th International Instrumentation Symposium, Albuquerque, New Mexico, May 21-23, 1974.
13. Richardson, M. and Potter, R., "Viscous vs. Structural Damping in Modal Analysis," 46th Shock and Vibration Symposium, San Diego, California, October 1975.
14. Savant, C. J., Jr., Basic Feedback Control Systems Design, McGraw-Hill, New York, 1958.
15. Shapton, W. R., "Use of Frequency Response in Determining the Transient Response of Complex Structures to Concentrated Loadings," PhD Dissertation, University of Cincinnati, 1968.
16. Simmons, D. J., "Finding Transfer Functions from Pulse Responses," Electronic Design, March 1964, pages 72-77.
17. Tse, F. S., Morse, I. E., and Hinkle, R. T., Mechanical Vibrations, McGraw-Hill, New York, 1958.

VITA

Clarence Walter Miller was born in North Charleroi, Pennsylvania, on March 14, 1947, the son of Mulford J. Miller (deceased), and Clara C. Miller. After graduation from Charleroi Area Senior High School, Charleroi, Pennsylvania, in 1965, he entered LeTourneau College in Longview, Texas. Upon completion of the Aviation Technician Program at LeTourneau, he entered the United States Air Force in 1968. In 1971, under the Air Force Airman Education and Commissioning Program, he entered the University of Texas at Austin. He received his Bachelor of Science in Aerospace Engineering from the University of Texas in 1973. In September, 1977, he entered the Graduate School of the University of Texas under another Air Force education program.

Permanent Address: 815 Parkview
Kilgore, Texas 75662

This Thesis was typed by Vickie Lynn Miller.